AERODYNAMIC PITCH-UP OF CRANKED ARROW WINGS: ESTIMATION, TRIM, AND CONFIGURATION DESIGN

by:

Alexander M. Benoliel

Thesis submitted to the faculty of the
Virginia Polytechnic Institute & State University
in partial fulfillment of the requirements for the degree of

Master of Science
in
Aerospace Engineering

APPROVED:

_____
William H. Mason, Committee Chairman

_____ _____
Bernard Grossman Mark R. Anderson

May 1994
Blacksburg, Virginia

AERODYNAMIC PITCH-UP OF CRANKED ARROW WINGS: ESTIMATION, TRIM, AND CONFIGURATION DESIGN

by

Alexander M. Benoliel

Committee Chairman: William H. Mason
Aerospace & Ocean Engineering

(ABSTRACT)

Low aspect ratio, highly-swept cranked arrow wing planforms are often proposed for high-speed civil transports. These wing planforms offer low supersonic drag without suffering greatly from low lift/drag ratios in low-speed flight. They can, however, suffer from pitch-up at modest angles of attack (as low as 5˚) during low-speed flight due to leading edge vortex influence, flow separation and vortex breakdown. The work presented here describes an investigation conducted to study past research on the longitudinal aerodynamic characteristics of highly-swept cranked wing planforms, the development of a new method to estimate pitch-up of these configurations, and the applications of this new method to the analysis of tail designs for trim at high lift coefficients. The survey of past research placed emphasis on 1) understanding the problem of pitch-up, 2) ascertaining the effects of leading and trailing edge flaps, and 3) determining the benefits and shortfalls of tail, tailless, and canard configurations. The estimation method used a vortex lattice method to calculate the inviscid flow solution. Then, the results were adjusted to account for flow separation on the outboard wing section by imposing a limit on the equivalent 2-D sectional lift coefficient. The new method offered a means of making low cost estimates of the non-linear pitching moment characteristics of slender, cranked arrow wing configurations with increased accuracy compared to conventional linear methods. Numerous comparisons with data are included. The new method was applied to analyze the trim requirement of slender wing designs generated by an aircraft configuration optimization and design program. The effects of trailing edge flaps and horizontal tail on the trimmed lift coefficient was demonstrated. Finally, recommendations were made to the application of this new method to multidisciplinary design optimization methods.

Acknowledgments

This work would not have been possible without the tireless efforts of my faculty advisor, Dr. William H. Mason. I would like to thank Dr. Mason and the other committee members, Dr. Bernard Grossman and Dr. Mark Anderson for their support and encouragement. A portion of this work was developed at NASA Langley Research Center and I would like to thank Dr. Harry Carlson, Dr. John Lamar, and Dr. Michael Mann for their help and suggestions in the theoretical analyses, the support of Mr. Peter Coen and the members of the Vehicle Integration Branch, the assistance of Mr. Kevin Kjerstad of the Subsonic Aerodynamics Branch, and Mr. David Hahne of the Flight Dynamics Branch. Also, Dr. Dhanvada Rao at Vigyan and Dr. William Wentz at the National Institute for Aviation Research were helpful in supplying me information on the experimental investigations of swept wing configurations, and Mr. Nathan Kirschbaum at Virginia Tech and Mr. Leroy Spearman at NASA Langley for their insight into the various supersonic transport programs conducted in the past. This work was supported by the NASA/Universities Space Research Association/Advanced Design Program (and the Vehicle Integration Branch at NASA Langley Research Center)

Table of Contents

List of Figures

Figure Page

Figure Page

List of Symbols

A	aspect ratio
α	angle of attack (measured in the wind axis coordinate system)
c	chord length
C_a	sectional axial force coefficient
C_D	total aircraft drag coefficient
C_l	sectional lift coefficient
C_L	total aircraft lift coefficient
$C_{l_{2D}}$	two dimensional lift coefficient
$C_{l_{max}}$	maximum two dimensional equivalent airfoil lift coefficient
C_{L_α}	lift curve slope, $\partial C_L/\partial\alpha$
C_m	sectional pitching moment coefficient
C_M	total aircraft pitching moment coefficient
C_n	sectional normal force coefficient
C_p	pressure coefficient
$\partial C_M/\partial C_L$	slope of pitching moment curve defining the stability of the aircraft
δ_{LE}	leading edge flap deflection in degrees (positive down)
δ_{TE}	trailing edge flap deflection in degrees (positive down)
δ_{Tail}	all moving horizontal tail deflection in degrees (positive down)
k	vortex lift factor
λ	taper ratio
Λ	wing sweep angle
M	Mach number
Re	Reynolds number
x	distance from the leading edge along the local chord of a particular wing section

1. Introduction to Low Aspect Ratio Planforms Designed for High-Speed Flight

Low aspect ratio wings with highly swept leading edges are the common choice for supersonic cruise transport aircraft configurations because of their low drag benefits in supersonic flight.[1] However, these planforms generally have poor low-speed aerodynamic characteristics such as low lift/drag ratios and low lift curve slopes, C_{L_α}. To compensate for the deficiencies of these wings, cranked arrow planforms are used in which a lower sweep outboard section is employed. This improves the low speed lift/drag ratio, increases the C_{L_α} and reduces the aerodynamic center shift from subsonic to supersonic flight conditions.[1] Unlike pure delta wings, at low speeds, these wings are susceptible to pitch-up in the high angle of attack flight regime. Pitch-up can occur at angles of attack as low as 5˚. Pitch-up is a result of non-linear aerodynamic effects, which include leading edge vortex flow, outer wing stall, and vortex breakdown. These effects are difficult to model with linear aerodynamic methods and continue to pose a challenge for CFD. It is important for configuration designers to be aware of the factors that can cause pitch-up and to determine the effectiveness of leading and trailing edge flaps in reducing pitch-up, providing adequate pitch control, and increasing low speed lift. Recently, Nelson[2] described the importance of non-linear aerodynamic characteristics in his study of High-Speed Civil Transport (HSCT) planform effects on off-design aerodynamics. Nelson noted that although highly swept arrow wing configurations were optimum for supersonic cruise performance, they suffered from low-speed, high angle of attack problems, such as pitch-up.

The airport noise problem also led researchers to study aerodynamically efficient, low speed, planforms to reduce required engine thrust, and thus takeoff noise. One of the reasons cited for canceling of the SST program in 1972 was community noise.[3] It is difficult to generate low drag lift for takeoffs and landings using a slender wing. This presents a challenge in designing an efficient high lift system capable of meeting the requirements of the HSCT.[4] The Concorde, with its slender wing, relied primarily on the lift generated by the leading edge vortex at high angle of attack to generate enough lift at low speeds. However, the drag penalty associated with the vortex lift resulted in a severe noise problem due to the required thrust for takeoff.[4]

This work describes an investigation conducted to review previous research done on high-sweep, low aspect ratio planforms and the current and past prediction methods developed. The goal of this work was to compile and assess past research, with emphasis

on understanding the pitch-up problem, determining the effectiveness of various leading and trailing edge flap configurations, understanding the benefits and shortfalls of tail, tailless, and canard configuration, developing an analysis method to estimate pitch-up using current linear aerodynamics codes, and applying this method to the determine the trim requirements of slender wings at high lift coefficients.

1.1 Past Research

Research on High Speed Civil Transport (HSCT) aircraft has been conducted for the past thirty-five years in the SCAT, SST, SCAR (SCR), and HSR programs.[3] Two configurations from the SCAT program that carried over to the SCAR program for further wind-tunnel testing were the SCAT-15F and SCAT 16. The SCAT-15F (Fig. 1a) was the fixed wing version of the SCAT-15 with leading edge sweep angles of 74˚, 70.5˚, and 60˚. The SCAT-16 (Fig 1b.) was a variable sweep configuration similar in design to the Boeing 2707-100,[3] which was Boeing's initial entry in the SST competition. Problems with this wing-tail configuration were exhaust scrubbing and acoustic noise/fatigue on the passenger cabin and aft fuselage; and pitch-up in both swept and unswept wing positions. The winning 1967 Boeing SST proposal 2707-200, while still a variable sweep wing design, reverted to a high sweep, low aspect ratio planform when the wing, in the most aft swept position, was integrated and locked onto the horizontal stabilizer. The four turbojets were mounted beneath the horizontal stabilizer exhausting behind the trailing edge. The resulting high-speed configuration was a classic slender delta with a long, overhanging forebody. Although Boeing won the SST contract with the 2707-200, they revised the design in 1969 into the fixed wing 2707-300 because there were overwhelming technical problems associated with the variable sweep wing design.[5] These problems included aeroelastic effects due to the long fuselage, the need for a canard to meet takeoff rotation requirements, low values of lift-to-drag ratio for loiter due to outboard panel stall, and main landing gear placement in relation to engine location.

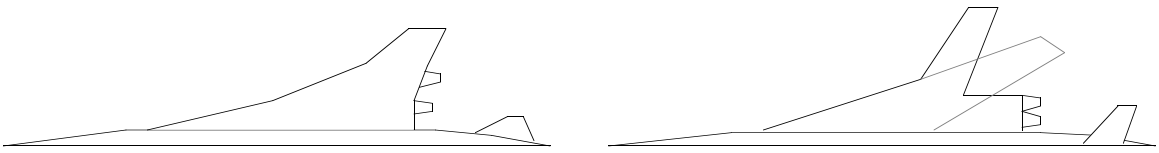

(a) SCAT-15F (b) SCAT-16

Figure 1. - SCAT Program developed configurations (not to scale).

During the SCAR program wind-tunnel tests were conducted to evaluate vortex flaps, blown flaps, and the effects of tail and engine placement[6-19]. A collection of key work is included in Tables B1 and B2 in Appendix B. Many of the early models tested were variations of the SCAT-15F design, and the Advanced Supersonic Technology (AST) series configurations evolved from this work. Other configuration design studies available on HSCT type concepts developed in the past are documented in reference 5 and 20 through 28.

2. Aerodynamic Pitch-Up

Pitch-up is defined herein as an abrupt change in slope of the $C_M(\alpha)$ curve such that the slope of the $C_M(\alpha)$ curve after the pitch break is greater than it was before the pitch break. The magnitude of the change in slope of the $C_M(\alpha)$ curve defining the pitch-up varies depending on the configuration. For some configurations it is mild and may be difficult to identify. An example of pitch-up is shown for a 71˚/57˚ sweep wing, tested by Yip and Parlett[19], in Fig. 2. The pitch break occurs at an angle of attack of about 6˚, corresponding to a lift coefficient of about 0.24. The figure includes a comparison with a vortex lattice numerical prediction method developed by Carlson, *et al.*[29] Note that the non-linear pitching moment occurs well within the operating regime of the aircraft and theory fails to predict it. Also, cranked arrow wings, such as the one shown in Fig. 2, are much more susceptible to pitch-up compared to pure delta wings.

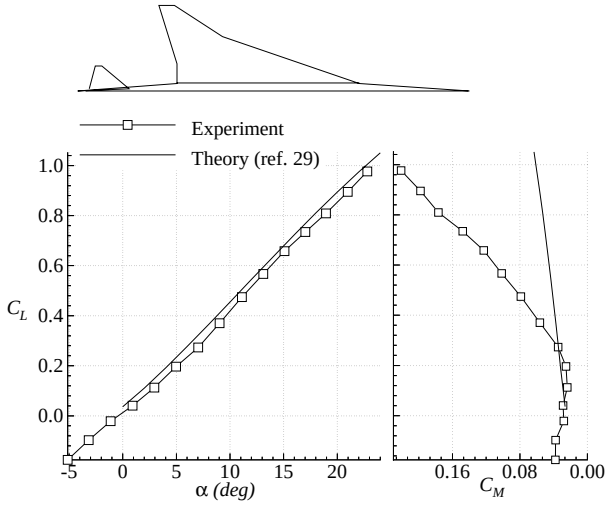

Figure 2. - Lift and pitching moment for a McDonnell Douglas 71˚/57˚ sweep cambered and twisted cranked arrow wing (ref. 19).

2.1 Theorized Reasons for Pitch-Up

For typical HSCT-class wings pitch-up is a result of the forces generated by the leading edge vortex inboard, together with flow separation and vortex breakdown on the outer portion on the wing. The strong effects of the leading edge vortex, and the loss of lift on the outboard wing sections due to flow separation, causes the center of pressure to move forward producing the pitch-up behavior. This is similar to the flow phenomenon

encountered on high aspect ratio swept wings.[30] The specific flow phenomenon which leads to the pitch-up distinguishes wing concepts. Some researchers believe that the pitch-up is a result of the vortex breakdown at the trailing edge, which progressively moves forward with angle of attack. It is likely, however, that the vortex may move away from the surface and lose influence before vortex breakdown occurs. This was identified in Lamar's discussion of experimental results.[31] It is more plausible that pitch-up is due to a combination of effects including vortex breakdown, but primarily due to outboard flow separation. It is important to identify if the pitch-up is dominated by the outboard flow separation or the strong inboard leading edge vortex, a function of the configuration.

Early work[32] was done to predict which types of configurations were susceptible to pitch-up to provide guidance for use in preliminary design. This work produced the well-known *DATCOM* design criteria for acceptable sweep and aspect ratio combinations. This method will predict if pitch-up will occur, although it does not define the angle of attack, or the lift level, where it will occur. It is also difficult to apply this method to cranked arrow planforms, in which more than one sweep angle is relevant.

A leading edge vortex on slender wings is created when the flow separates at the leading edge and then reattaches downstream on the surface, creating an area of low pressure above the leading edge on the upper surface (Fig. 3). As the angle of attack is increased, the core of the main vortex moves inboard[11,34] and remains coherent up to larger angles of attack for higher sweep wings as shown by Wentz and Kohlman.[35]

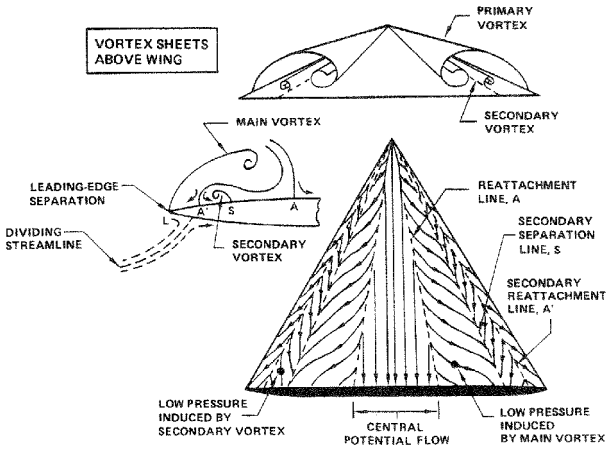

Figure 3. - Leading edge vortex features on highly swept wings (ref. 33).

For a cranked arrow wing, two vortex systems may be formed due to the leading edge flow separation on each wing section. The inboard vortex can extend into the aft

portion of the outboard wing section. It also induces an upwash on the outboard wing section. The flow incidence angle on the outboard portion of the wing is considerably higher than the aircraft angle of attack due to this upwash. At low angles of attack, the vortex flow on the outboard wing section increases the longitudinal stability. This result is due to the fact that the outboard wing section is aft of the center of gravity, thus contributing a nose down moment. As the angle of attack increases, the outboard vortex system breaks down. At the same time, the inboard system moves further inboard, thus unloading the outboard wing section, as shown by Coe, *et al*.[8,10] Rao[36] also studied this outboard vortex breakdown in a test of a 70˚/50˚ sweep flat cranked delta wing. Through oil flow and smoke visualization, he showed the onset of vortex breakdown and flow separation on the outer wing panel at angles of attack as low as 5 degrees. This loss of lift on the outboard portion of the wing in conjunction with the strong inboard leading edge vortex causes pitch-up on slender arrow wings. The particular wing concept determines if flow separation on the outboard wing panel or the inboard leading edge vortex will initiate the pitch-up.

2.2 Influence of Geometry on Pitch-Up

Several factors affect the pitch-up behavior of cranked arrow wing planforms. The introduction of a trailing edge notch places greater demands on the wing leading edge region. This effect is clearly seen in arrow wings with increasingly large trailing edge notches as shown in Fig. 4 taken from Poisson-Quinton.[37] As the angle of attack is increased, the wing-tips become unloaded and the vortex core moves inboard. With the large trailing edge notches, the vortex has less area aft to affect, causing a destabilization in the longitudinal stability. Note that the pure delta wing does not encounter pitch-up.

The size of the trailing edge notch of an arrow wing can dramatically affect the pitch-up behavior of highly swept wings. It was shown by Grafton[38] that the addition of a trailing edge extension on a modified arrow wing planform (Fig. 5a) reduced pitch-up (done as part of the F-16XL planform development program). Although this modification did not change the angle of attack for pitch-up, it did reduce the severity of the pitch-up, as shown in Fig. 5b. Grafton also found major effects resulting from a leading edge notch on the same model. Here, the leading edge notch weakened the leading edge vortex[38], resulting in a reduction of the severity of the pitch-up. This result demonstrates the possible sensitivity of pitch-up and lift characteristics to small planform changes brought about if these small changes produce a fundamental change in the leading edge vortex.

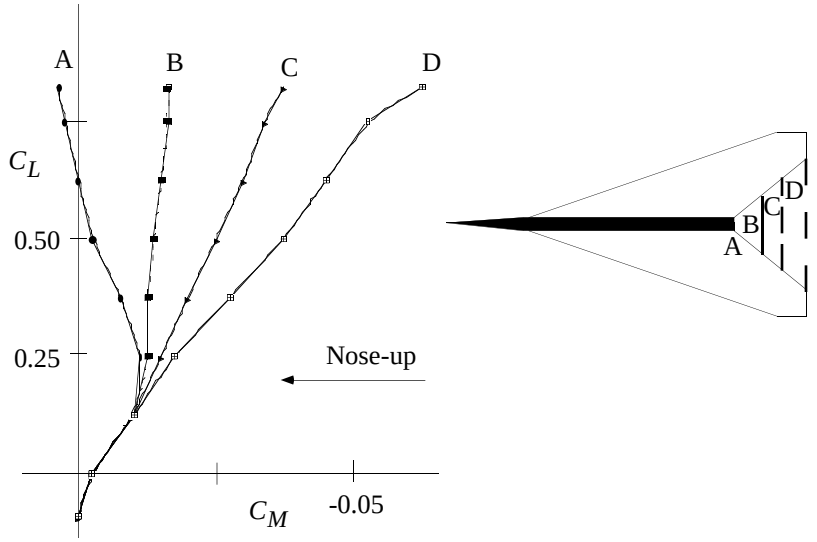

Figure 4. - Variation of pitching moment for a 75˚ sweep arrow wing with varying trailing edge notches (ref. 37).

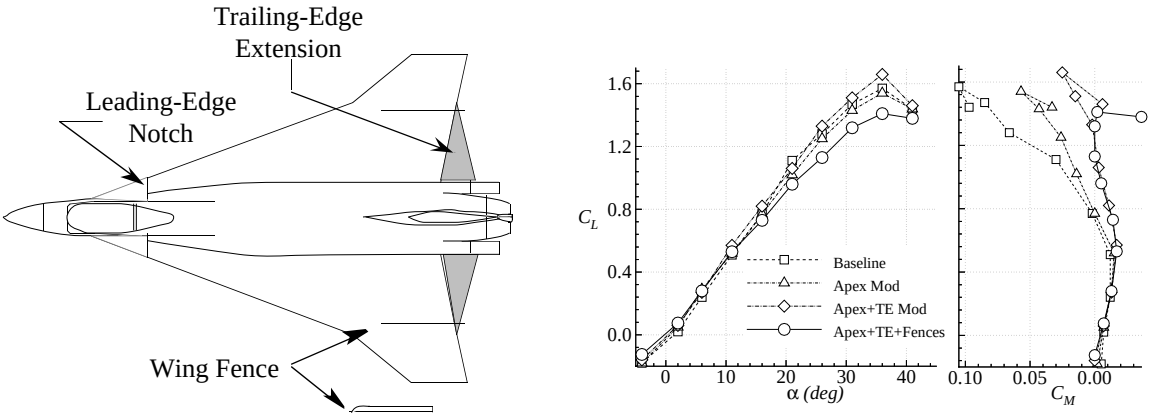

(a) Model diagram with trailing edge extension, leading edge notch, and wing fence.

(b) Lift and pitching moment data for several configurations (ref. 38)

Figure 5. - Modified F-16XL predecessor model

Much like the leading edge notch, the shape and incidence of the leading edge can affect the vortex lift. Increasing the leading edge radius has the effect of improving the longitudinal characteristics by retarding the formation of the leading edge vortex.[12,13,16,33] This also reduces the vortex lift, as shown in Fig. 6. The local angle of attack of the leading edge seems to have the greatest effect on the aerodynamic characteristics with respect to the pitch-up. To minimize the formation of the vortex, it is desirable to deflect the leading edge

such that the leading edge incidence relative to the local flow angle of attack at each spanwise station is zero. Then, at angles of attack above this condition, the vortex will be formed uniformly. The leading edge can also be shaped and deflected such that the leading edge vortex is maintained on this surface.[39] Applying this concept to a leading edge device results in the so-called *vortex flap.* Generally used for transonic maneuverability, deflecting the leading edge allows for the development of vortex lift while recovering some of the leading edge-suction to reduce drag.[39] The vortex flap shape and wing camber must be optimized for minimum lift-induced-drag to be effective. The effects of leading and trailing edge flaps will be discussed in more detail in the following section.

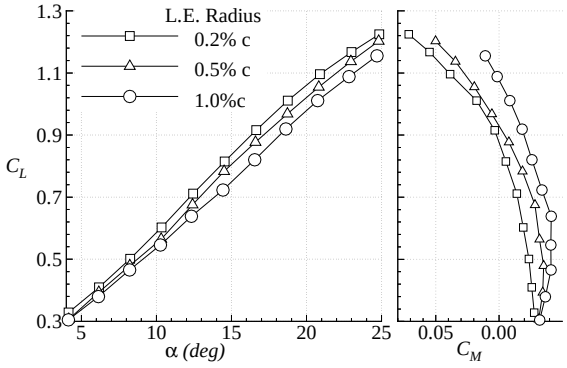

Figure 6. - Effect of leading edge radius on lift and pitching moment on the SCAT-15F (ref. 16)

Planform effects, such as the outboard wing sweep, were studied by Hom, Morris, and Hahne.[40] Hom, *et al*, theorized that the pitch-up was a result of flow separation on the outboard wing panel, a function of the spanwise flow, and vortex breakdown. Four models were tested with a 70˚ sweep inboard wing section and varying outboard wing sweeps ranging from 60˚ to -20˚. They found that the lower sweep outboard wing panels encountered less spanwise flow and thus, the flow remained attached on the outboard panels. As the outboard sweep angle was increased, the flow on the outboard wing section separated and became dominated by a leading edge vortex on this section. The angle of attack for pitch-up was found to be unaffected by the outboard wing sweep. However, helium bubble flow visualization techniques showed that the cause of the pitch-up varied for the cambered and uncambered wings. It was found that the pitch-up for the uncambered wings was due to vortex breakdown at the trailing edge. When leading and trailing edge flaps were

deflected (to postpone the formation of the leading edge vortex) the pitch-up was a result of basic flow separation on the outboard wing section and not vortex breakdown.

Some of the configurations developed such as the SCAT-15F, the AST-100 and AST-200 series, and the General Dynamics F-16XL, incorporate the use of vertical fins or fences located outboard on the wings (generally placed at the crank location). Grafton[38] found that the effect of fences located just inboard of the wing crank on a predecessor of the F-16XL (Fig. 5a) reduced the lift and created a slight improvement in the pitch-up at high angles of attack as shown in Fig. 5b. In a later test of a similar model, Grafton and Nguyen[41] found that the slope of the pitching moment curve after the pitch-up increased with the addition of the wing fences at moderate angles of attack (decreasing longitudinal stability), and improved the longitudinal stability slightly at high angles of attack. Lockwood[13] tested a modified SCAT-15F model and found that vertical fins (whether located at the crank or inboard of the crank) reduced the longitudinal stability as well as the lift. This result is contradictory to Grafton and Nguyen's findings. Both researchers agreed, though, that the effects were likely due to the loss of vortex influence on the outboard wing section and vortex breakdown due to the presence of the fences. Another effect of the fences or fins in these tests was to cause the inboard vortices to break down symmetrically in side-slip, thus improving lateral stability.[13,38]

2.3 Further Considerations

The formation of the leading edge vortex has been shown to be affected by Reynolds number. Furlong and McHugh[42] addressed the effect of Reynolds number in their summary of the aerodynamic characteristics of swept wings. They showed that the effect of Reynolds number on the leading edge flow separation was more prominent for wings with airfoil sections having rounded leading edges than sharp leading edges (Fig. 7). The "inflection" lift coefficient used in Fig. 7 refers to the lift coefficient at which there is an increase in lift coefficient due to the formation of a leading edge vortex.

The insensitivity of vortex flow to Reynolds number effects has been shown by a variety of researchers by analysis of force data taken from tests of HSCT plan-forms[14,16,17, 37,43]. The variation of Reynolds number for these tests were on the order of about one magnitude. However, Re and Couch[16] found that Reynolds number variations during the testing of a SCAT-15F model did affect the measured forces. They found that longitudinal stability decreased with increasing Reynolds number for the configuration equipped with an unswept canard. This effect was found to be a result of the sensitivity to

Reynolds number of the flow over the canard only and not the wing. Contrary to these results, Furlong and McHugh[42] found that Reynolds number effects were small on straight surfaces and more prominent on swept wings. Malcolm and Nelson[44] found that Reynolds number variation affected the position and interaction of the vortex cores in their study of a cranked fighter wing configuration dominated by vortex flow. These effects cast doubt on the validity of low Reynolds number results for wings with cranks or curved leading edges.[45]

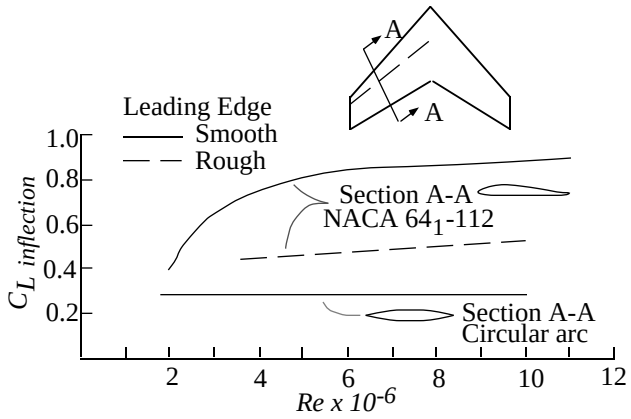

Figure 7. - Effects of Reynolds number on the inflection lift coefficient for wings incorporating round and sharp leading edges. $\Lambda_{c/4} = 50^{\circ}$; A = 2.9; λ = 0.625 (ref. 44).

Another factor of concern is the possible effect of the testing techniques used. It was shown by Johnson, Grafton, and Yip[46] that obstacles behind the model, such as a strut, can significantly affect the vortex burst angle of attack and thus the measured forces. Wentz and Kohlman[35] also found similar results in their investigation of vortex breakdown.

2.4 Pitch-Up Alleviation

Other than deflecting the leading edge, few active intervention methods have been developed to reduce or postpone pitch-up behavior. One method is the Pylon Vortex Generator (Fig. 8) investigated by Rao and Johnson.[47] The Pylon Vortex Generator creates a streamwise vortex with a rotation opposite that of the leading edge vortex, such that it creates a downwash outboard of the vortex generator. This downwash reduces the effective angle of attack on the outboard wing section to postpone flow separation. The effect of the device is to create nose-down pitching moments at high angles of attack without a large

drag penalty. Rao and Johnson tested the device on a 74˚ sweep flat plate delta wing with sharp leading edges at subsonic speeds. The effects of the device on pitching moment are shown in Fig. 9 for the vortex generator design shown in Fig. 8 (several designs were tested). Although the severity of pitch-up that this wing experienced was comparatively small (see Fig. 2), the device made a difference. The Pylon Vortex Generator was incorporated in the configuration design of the AST3I Mach 3.0 supersonic transport.[26] On the AST3I, the vortex generator was incorporated into a leading edge notch-flap and was located at the wing crank location. A model of this configuration was tested in a water tunnel to investigate the vortex patterns. Flow visualization studies showed the device created a counter-rotating vortex over the outboard wing section as found by Rao in his investigation.

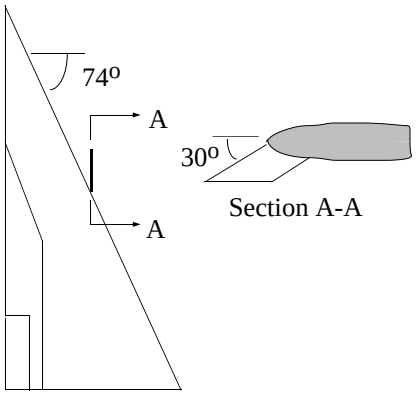

Figure 8. - Pylon Vortex Generator Design (ref. 47).

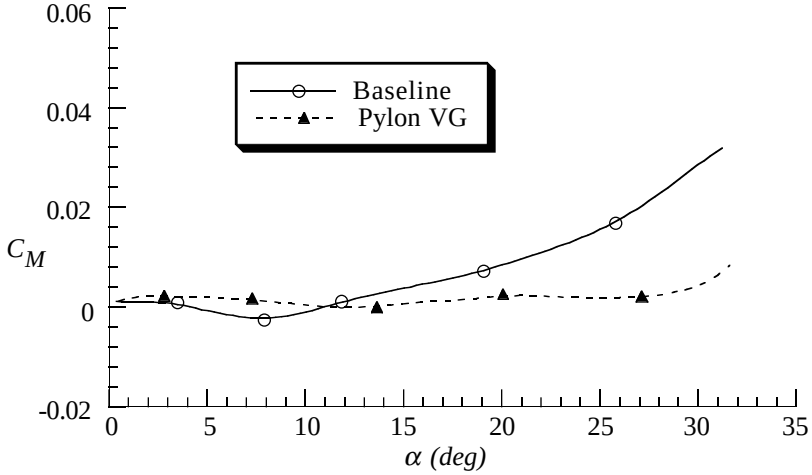

Figure 9. - Pylon Vortex Generators at 25% and 50% chord (ref. 47).

The Pylon Vortex Generator is similar to an engine pylon and the benefits of the device to the longitudinal stability are similar to those described by Shevell for the DC-8.[48] It was found that the presence of the engine pylons postponed stall on the outboard wing section of the Douglas DC-8, thus improving the pitching moment characteristics in the stall region. The aft engine DC-9 suffered from similar longitudinal instability problems as the DC-8, but did not have wing mounted engines to alleviate spanwise flow at stall conditions. Engineers experimented with the DC-9 by installing engine pylons on the wings to improve the longitudinal stability of the aircraft in much the same way as they did with the DC-8. The spanwise placement of the device was such that the trailing vortices from the pylons created an upwash on the high horizontal tail, creating a nose-down moment. The pylons were reduced in size, streamlined, and patented as *vortilons* (vortex generating pylons) and incorporated on all DC-9 aircraft[48].

Another means of controlling the pitch-up is spanwise blowing on the outboard wing section. Bradley, Wray and Smith[49] tested the effects of blowing on 30˚ and 45˚ sweep delta wings to augment the leading edge vortex. This technique was incorporated by Rao in the test of a 70˚/50˚ sweep uncambered, untwisted wing[36]. The model tested incorporated a chordwise blowing slot which exhausted over the outboard section of the wing (Fig. 10). The intent of having a jet of air blown over the outboard wing section was to maintain a stable vortex core, thus producing lift and preventing vortex breakdown from occurring. Results of the test by Rao are shown in Fig. 11. The investigation of this technique revealed marked improvements in postponing the pitch-up behavior and allowed for increased aileron effectiveness for roll control at high angles of attack for a range of $c\mu$ = 0.01 to 0.02. However, this test was performed at a relatively low Reynolds number (Re = 0.8×10^6). Further testing is required to validate the concept.

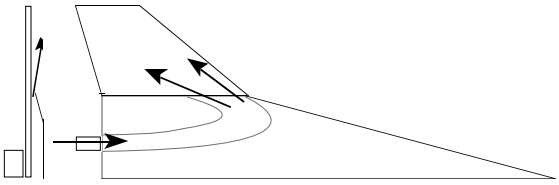

Figure 10. - Spanwise blowing study 70˚/50˚ sweep model (ref. 36).

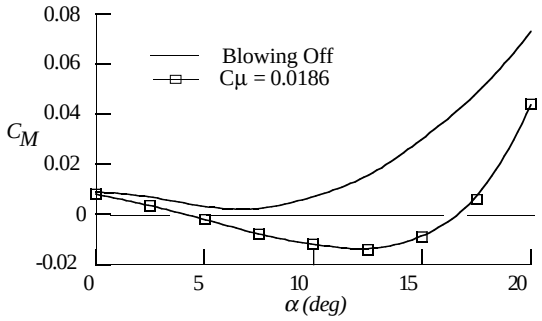

Figure 11. - Effect of spanwise blowing on a cranked delta wing (ref. 36).

3. High-Lift for Slender Wings

3.1 Leading Edge Flap Effects

The effect of leading edge flap deflection is to postpone the formation of the leading edge vortex and classical flow separation. This effect is accomplished by deflecting the control surface to an angle such that the local leading edge incidence to the oncoming flow is zero.[8] As shown in Fig. 12, the effect of deflecting the leading edge flap for an uncambered, untwisted wing with a uniform flap deflection of 30˚ is to postpone the pitch-up behavior while reducing the lift. Coe, *et al*[11] showed that the effects for a cambered and twisted wing with the same leading edge-flap deflection were to change the zero angle of attack lift and pitching moment and had only a small effect on the pitch-up behavior. This was due to the fact that the pitch-up for this configuration was dominated by the influence of the strong inboard vortex.

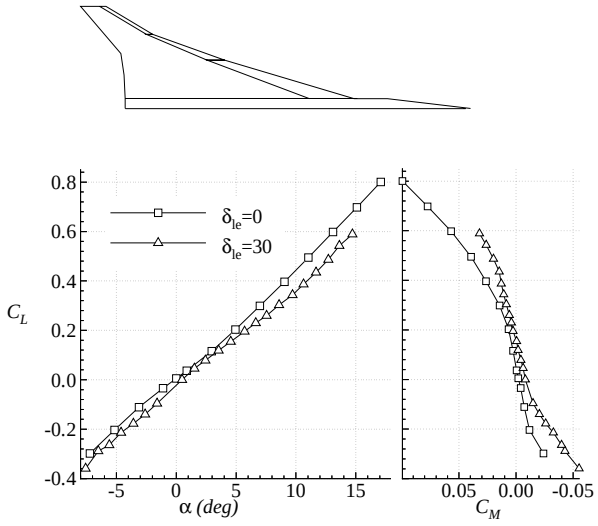

Figure 12. - Effect of leading edge flap deflection for a 74˚/70.5˚/60˚ sweep untwisted, uncambered cranked arrow wing similar in planform to the AST-200. (ref. 11).

Several studies have investigated the optimization of flap deflections with the use of multi-segmented flaps to allow for the flow incidence relative to the leading edge to be approximately zero along the entire span. Coe, Huffman, and Fenbert[10] found that using a continuously variable leading edge deflection had a favorable effect on the lift/drag ratio compared to an uniformly deflected flap. This effect was only realized if the leading edge

flap was smoothly faired aerodynamically, which would be difficult mechanically. No significant improvement in the pitch-up characteristics was found for segmented flap compared to the uniformly deflected flap. Fairing the flap had little effect on the lift and pitching moment. Furthermore, the unfaired segmented flap had higher drag values than the faired flap and the uniformly deflected flap, most likely due to the discontinuity between each flap segment.[10] The effects of the faired multi-segmented flap are shown in Fig. 13 for a cambered and twisted model. Yip and Parlett[19] also tested the effects of deflecting a multi-segmented leading edge flap and presented results for a variety of combinations of flap deflections. They found that deflecting the leading edge did not change the angle of attack at which pitch-up occurred, but it did reduce the magnitude of the pitch-up.

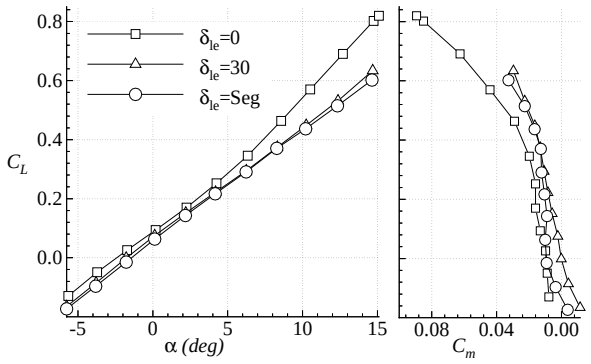

Figure 13. - Effects of a multi-segmented flap for a 74˚/70.5˚/60˚ sweep cambered and twisted cranked arrow wing planform (ref. 10).

3.2 Trailing Edge Flap Effects

Trailing edge flaps are used to produce both an increment in lift and pitching moment. If leading edge flaps are used for low-speed, high angle of attack flight, it is desirable to deflect the trailing edge flaps to recover the lost vortex lift. Due to large root chords on HSCT planforms, trailing edge flaps are often of small chord lengths compared to the local chord, thus limiting their performance. Prediction of trailing edge flap performance becomes critical when designing for adequate control power. Wolowicz and Yancey[50] showed that available elevator control power during landing was an issue of concern during flight tests of the North American Rockwell XB-70 aircraft. They found that the actual required deflection angles to trim at landing were approximately 4˚ higher than the predicted values. During one landing the elevator had to be deflected to the maximum down position to trim.

Quinto and Paulson[51] studied the effects of leading and trailing edge deflection of flaps on the aerodynamics of a 70˚/48.8˚ sweep uncambered, untwisted wing. As shown in Fig. 14, the effects of the trailing edge flap deflection are to shift the lift curve in a positive direction and the pitching moment curve in a negative direction. It can be seen in Fig. 15 that the effect of flap deflection is not linear and the effectiveness decreases with an increase in the angle of attack for the lift. The flap effectiveness for the pitching moment was fairly linear throughout the angle of attack range tested.

The effectiveness of the trailing edge flaps are also dependent on the leading edge contour. Coe and Weston[8] found that trailing edge flap effectiveness increased when the leading edge flap was properly deflected such that flow conditions at the leading edge were improved and the flow was attached at the trailing edge. McLemore and Parlett[43] found that the effectiveness of the outboard trailing edge flaps was small due to the flow separation on the outboard wing panel. This will impact the roll control concept of the aircraft.

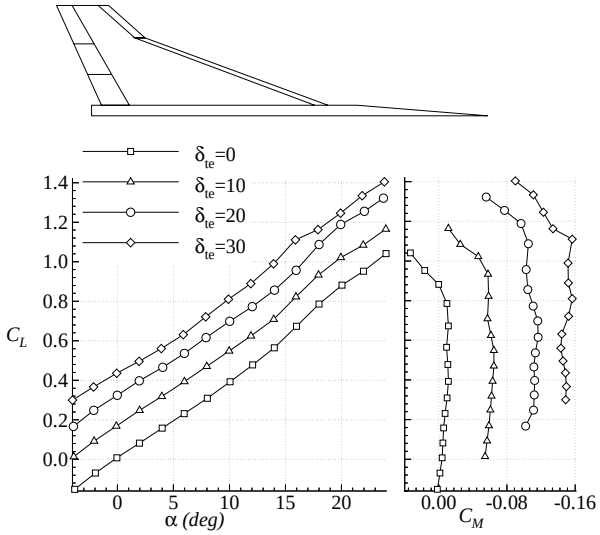

Figure 14. - Trailing edge flap effectiveness for a 70˚/48.8˚ sweep uncambered, untwisted cranked arrow wing planform with δ_{LE} = 20˚ (ref. 51).

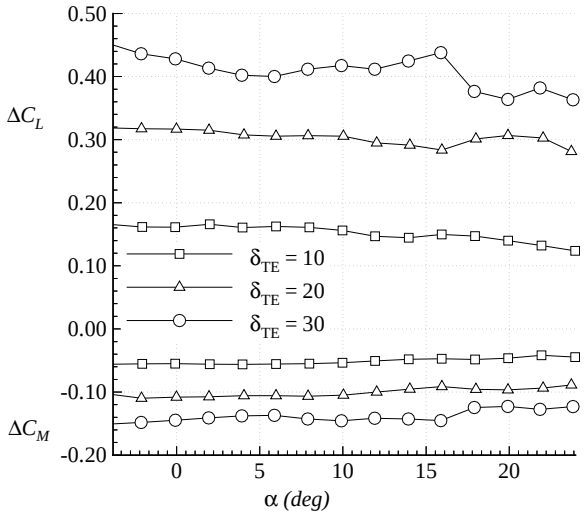

Figure 15. - Increments in lift and pitching moment for various trailing edge flap deflections for a 70˚/48.8˚ sweep flat cranked arrow wing (ref. 51).

4. Theoretical Estimation Methods

Estimation methods used to date that are of relatively low computational time and cost are linear aerodynamic methods. These methods work quite well in the linear aerodynamic range but, as expected, do not accurately predict the aerodynamic forces and moments in relatively high angle of attack regimes where non-linear aerodynamics (i.e. vortex interaction, vortex burst, and basic flow separation) plays an important role. As shown above, high-sweep, low-aspect ratio configurations can experience non-linear aerodynamic effects at rather low angles of attack, thus reducing the accuracy of basic codes even further.

To increase the prediction accuracy, these codes can be modified to incorporate some type of vortex effect.[29,52] A common method used for predicting the effects of leading edge vortices is through the use of variations on the Polhamus suction analogy.[34,53, 54] The premise behind these methods is that for separated flow around the leading edge of a swept wing, the additional normal force due to the suction pressure under the vortex is related to the leading edge thrust for attached flow. The calculated axial leading edge suction force is rotated such that it is normal to the surface. This suction can then be integrated along the span to determine the overall contribution of the leading edge vortex to the lift and drag. Empirical correlation can also be used to locate the position of the vortex core and distribute the contribution chordwise, rather than applying it at just one chordwise point on each spanwise station, to improve the accuracy in the calculation of the moments.[53] The contribution of the side edge vortex can be calculated in a manner similar to the leading edge force determination.[55] The side edge force can become an important factor for highly swept wings with large tip chords.

Harry Carlson[56,57] has improved the accuracy of prediction methods by using data-theory correlation to estimate the actual *attainable thrust* of the leading edge taking into account local viscous effects. The method, developed for drag prediction with partially separated flow, calculates the attainable thrust and then applies the remaining thrust as vortex lift through the suction analogy. This method has been employed for wings with leading and trailing edge flaps, and in combination with canard and tail configurations.

With the current linear theory methods available, the contribution of vortex lift can be calculated with relatively good accuracy for many configurations. However, the vortex lift imparted on some planforms, such as cranked arrow planforms, is due to a complex system of multiple vortices which are difficult to model accurately. Current methods do not

predict the vortex loss of influence due to travel away from the surface, core breakdown, the interaction between vortex systems, or, of course, classical separated flow.

4.1 A New Method to Estimate Pitch-Up

To estimate the pitch-up of cranked arrow-wing planforms, a study was conducted on a number of planforms that exhibited pitch-up during experimental investigations. These results were used to develop a new estimation method. A variety of planforms were modeled and studied with the vortex lattice estimation method, *Aero2s*, developed by Carlson.[29,53] Section lift coefficients were plotted for each spanwise station at angles of attack near the pitch-up regime. The lift coefficients were converted to equivalent two-dimensional values using:

$$C_{l_{2D}} = \frac{C_l}{cos^2 \Lambda_{ref}} \tag{1}$$

where C_l is the 3-D sectional lift coefficient at a particular span station and Λ_{ref} is the reference sweep angle at that span station. For this method, the reference sweep is chosen to be the mid-chord sweep angle. The vortex lattice code used calculates the normal and axial forces at each spanwise station by integrating the pressures. The sectional lift coefficient can then be calculated by:

$$C_l = C_n cos\alpha - C_a sin\alpha \tag{2}$$

where C_n and C_a are, respectively, the 3-D sectional normal and axial force coefficients. The vortex lift and leading edge thrust effects were unchanged.

The 2-D lift coefficient distribution for a McDonnell Douglas Supersonic Transport model (Fig.2) is shown in Fig. 16. The large 2-D lift coefficients at the inboard stations are due to the modeling of the fuselage with a large leading edge sweep angle. Note, from Fig.2, that the pitch-up occurs at about 6˚ angle of attack. If a 2-D sectional lift coefficient limit of 0.85 is chosen, it can be seen that part of the outboard sectional lift is in excess of this value at angles of attack beginning at about 6˚. This maximum lift value was picked because it is close to the actual airfoil maximum lift coefficient of the 3% thick airfoil section used for the outboard wing panel.

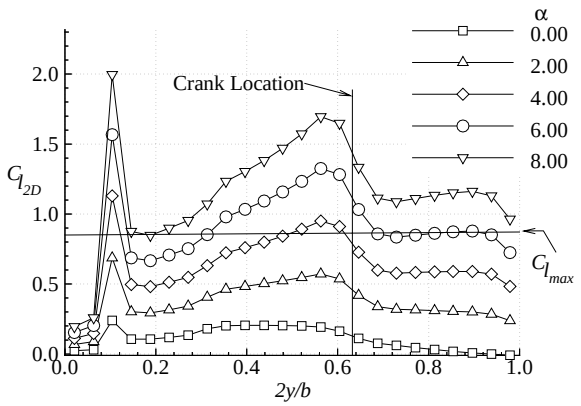

Figure 16. - 2-D sectional lift coefficient for a 71˚/57˚ sweep wing calculated with *Aero2s*.

Thus, it is proposed to use the equivalent 2-D section lift limit to model separated flow on the outboard panel. To estimate the outboard wing panel flow separation, a limit is imposed on the outboard section lift coefficient in the calculation of the total aircraft forces and pitching moment. This limit is chosen to be the maximum two-dimensional lift coefficient for the airfoil section of the outboard wing panel. The selection of this limit will be discussed later in this chapter. The sectional normal force on the outboard wing section is limited to a value such that it does not exceed the prescribed maximum 2-D lift coefficient, $C_{l_{max}}$. Once the 2-D lift coefficient, as calculated in Eq. 1, exceeds the maximum 2-D airfoil lift coefficient, the correction to the 3-D sectional normal force coefficient can be made with the following equation:

$$C_{n_{Corrected}} = \frac{(C_{l_{max}} cos^2 \Lambda_{ref} + C_a sin\alpha)}{cos\alpha} . \qquad (3)$$

The total aircraft lift and pitching moment will now include a loss of lift on the outboard wing section. A similar method for estimating the maximum lift coefficient of swept wings from straight wing data was proposed by Hoerner.[58]

The calculation of the pitching moment does not, however, account for the aft shift in the center of pressure due to the stalled flow pattern. The corrected 3-D pitching moment is calculated from the Eq. 4 below:

$$C_{m_{Corrected}} = C_m \frac{C_{n_{corrected}}}{C_n} \qquad (4)$$

where C_m and C_n are, respectively, the original 3-D sectional pitching moment and normal force coefficients. The total aircraft pitching moment coefficient is calculated by:

$$C_M = \frac{1}{N} \sum_{j}^{N} C_{m_j} \frac{c_j}{c_{ave}} \tag{5}$$

where N is the total number of spanwise stations, C_{m_j} is the 3-D sectional pitching moment at section j (after the correction has been applied, if required), c_j is the local chord at section j, and c_{ave} is the average chord over the span. Leading edge thrust and vortex lift effects are then added to this result to determine the final value of the pitching moment. The lift is calculated in a similar manner.

4.2 Results

The cambered and twisted configuration presented in Fig. 2 is presented again in Fig. 17 with the results of the new Aerodynamic Pitch-up Estimation (APE) method. A maximum airfoil lift coefficient of 0.85 was chosen for the 3% thick outboard wing section. The results of the new method are shown with a solid line, labeled as Aero2s + APE. The new method estimates the pitch-up well, although it does not estimate the lift coefficient as accurately. At a lift coefficient of 0.6, the difference between experiment and the APE method is about 0.07.

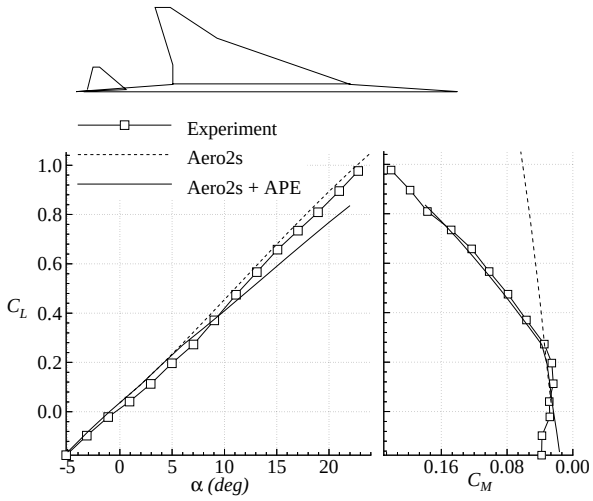

Figure 17. - Comparison of lift and pitching moment estimation methods for a 71˚/57˚ sweep cambered and twisted cranked arrow wing (δ_{Tail} = 0˚).

When the method was applied to the aerodynamic assessment of a uncambered, untwisted wing configuration, the results were even more promising. The configuration shown in Fig. 18 is a flat, cranked arrow wing tested by Kevin Kjerstad (the data is from a yet to be published NASA TP). This model was part of a family of arrow wings tested by Kjerstad. The wings are flat plates of constant absolute thickness, with beveled leading and trailing edges. Inboard and outboard leading edge sweep angles are 74˚ and 48˚ respectively. A maximum airfoil lift coefficient of 0.75 was chosen.

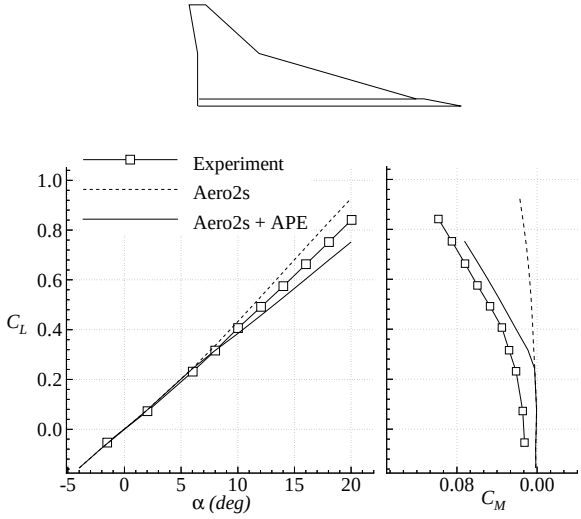

Figure 18. - 74˚/48˚ sweep wing-body combination, comparison to experimental data.

The pitch-up of this configuration is not as severe. The APE method also does a better job at estimating the lift. At a lift coefficient of 0.6, the difference between the new method and experiment is about 0.03. The small non-zero pitching moment at zero lift was presumably due to a camber effect created by the beveled leading edge not modeled in the aerodynamic analysis.

The results for an F-16XL model tested by David Hahne (from an unpublished test) are shown in Fig. 19. This model incorporated a 70˚/50˚ sweep, cambered and twisted, cranked arrow wing. The data shown is for the model configured for an HSCT type planform. A maximum 2-D airfoil lift coefficient of 0.80 was chosen for the biconvex airfoil section of the outboard wing panel.

The new estimation method results indicate good agreement with the experimental data. The pitching moment curve slope was estimated with relatively good accuracy before

and after the pitch-up region, although the method failed to predict the angle of attack at which pitch-up occurred. As in the previous case, a discrepancy existed between the zero-lift pitching moment estimated by the VLM code and the experimental data. The likely cause for this discrepancy is that the aircraft fuselage was not modeled with enough accuracy to estimate the pitching moment at zero lift.

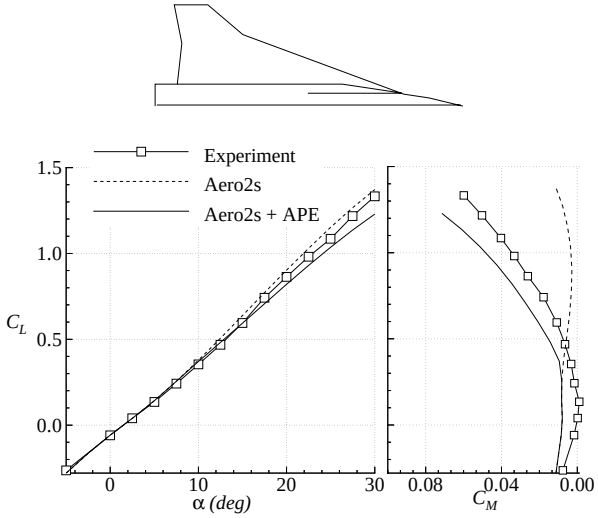

Figure 19. - Comparison of estimation methods for an F-16XL (70˚/50˚ sweep) model test.

4.2.1 Leading Edge Vortex Considerations

The pitch-up of the cases presented thus far was due primarily to the flow separation on the outboard wing panel, outboard vortex breakdown, or a combination of the two effects. A case in which the pitch-up is due primarily to the strong inboard leading edge vortex is exemplified in a test by Coe[11], shown in Fig. 20. The slender and highly swept, uncambered, untwisted, 74˚/70.5˚/60˚ sweep configuration promotes a strong inboard leading edge vortex which has little effect on the outboard wing section. A weak leading edge vortex also forms on the outboard section, although the flow on this section separates early.[10] When this is the dominant flow mechanism, the original Carlson method (*Aero2s*) did a better job at estimating the pitching moment than the modified method. Now an investigation is conducted to explain these results.

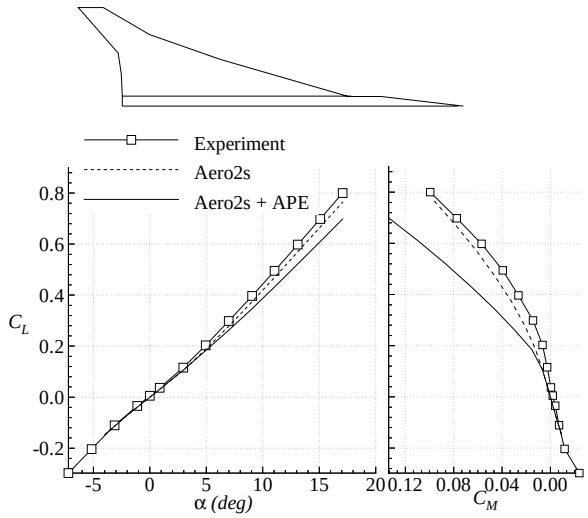

Figure 20. - Comparison of lift and pitching moment estimation methods for a 74˚/70.5˚/60˚ sweep uncambered and untwisted cranked arrow wing similar in planform to the AST-200.

The VLM code used in this study uses an empirical estimate of the location of the leading edge vortex as a function of local leading edge sweep angle, angle of attack, and the location of the apex of the vortex (generally set to the wing root of the configuration). A sinusoidal vortex pressure distribution as a function of local chordwise position is used for each spanwise station:

$$\Delta Cp_{vortex}(x) = k(1 - \cos \pi \frac{x}{x_{vor}}) \qquad (6)$$

where x is the chordwise position and x_{vor} is the chordwise position of the vortex core, both measured aft of the leading edge. The value of x ranges from zero to two times the value of x_{vor}. Thus, the vortex induced pressure distribution starts at the leading edge and peaks at the vortex core position. The value of k is such that the integrated area of the entire distribution is equal to the vortex lift calculated using the Polhamus suction analogy and the attainable thrust relations. If the local chord length is greater than $2 \bullet x_{vor}$. then only part of the vortex force is applied (Fig. 21).

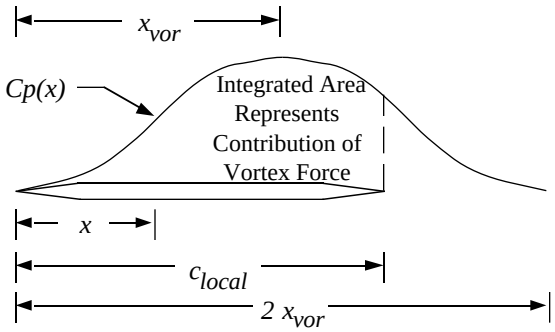

Figure 21. - Pressure distribution used to calculate the contribution of vortex lift.

The vortex placement estimates for the configuration shown in Fig. 20 are shown in Fig. 22, compared to the experimental results found by Coe.[11] The code does not distinguish between two vortex systems and simply uses a continuous vortex whose position changes depending on the local sweep angle. For this configuration the inboard and outboard sweep angles are both large, thus the leading edge vortex, estimated by the code, has only a small effect on the outboard wing panel at high angles of attack. Note that the code extends the vortex to the nose of the aircraft. *Aero2s* assumes that vortex lift acts across the entire span, including the fuselage region. The vortex apex location specifier does not limit the vortex from acting inboard of that position.

The method can be refined by limiting the vortex effects to the wing only, and eliminating the contributions to the sectional characteristics of the fuselage. When this correction is applied a very different result for the pitching moment compared to Fig. 20 is found (Fig. 23). This refinement will be called the “limited vortex” modification. For the limited vortex modification shown in Fig. 23, the vortex is begun at the wing root.† Note that the new estimation method now becomes more accurate in predicting the pitching moment. This is because the long moment arm that the vortex force has in the fuselage region has been eliminated.

† A sensitivity of calculated vortex forces to the amount of grid points used was found. This was a results of the increased resolution obtained with a larger number of spanwise stations. The increased number of grid points offered only a small change in the inviscid solution.

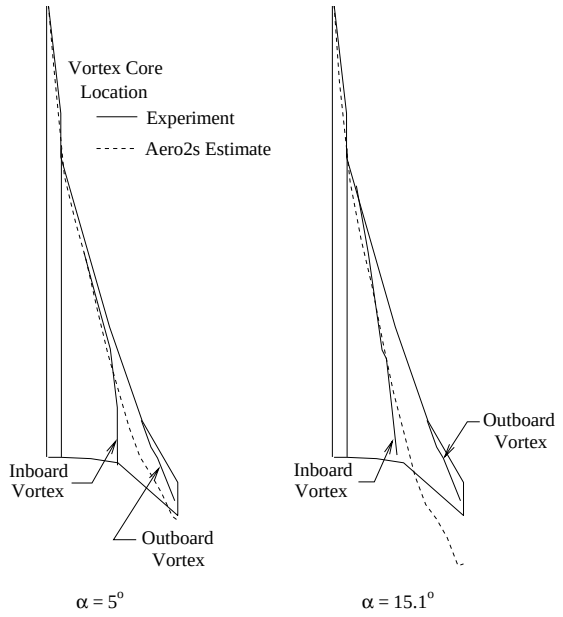

Figure 22. - Vortex placement comparison between theoretical estimates and experiment.

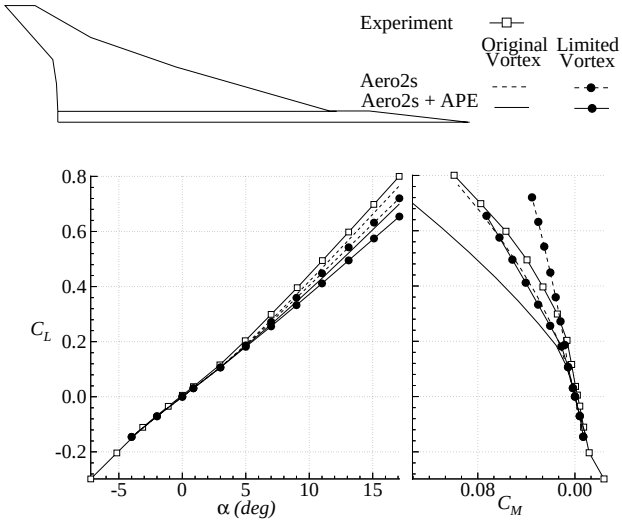

Figure 23. - Effects of limiting the vortex effects to the wing only for a 74˚/70.5˚/60˚ sweep wing similar in planform to the AST-200. Limited vortex begins at wing root and does not extend into fuselage region.

When this correction to the vortex location was applied to the previously presented cases, only a small change in the results was found. This was due primarily to the fact that the pitch-up of these configurations was due to flow separation on the outboard panels rather than the strong leading edge vortex. The lower leading edge sweep angles of the

previously studied configurations allowed for the leading edge vortex to have a greater effect on the outboard wing panels. These cases had inboard sweep angles ranging from 68˚ to 71˚, and outboard sweep angles ranging from 48˚ to 57˚, compared to the 74˚/60˚ sweep angles of the AST-200 configuration in question.

It is also possible that the vortex system developed is such that it does not promote pitch-up at low angles of attack. The theoretical and experimental results for a 70˚/48.8˚ sweep configuration tested by Quinto and Paulson[51] are shown in Fig. 24 without the correction to the leading edge vortex. This is a flat wing configuration which uses an NACA 0004 airfoil section for the entire wing. A maximum airfoil lift coefficient of 0.90 was chosen. For this case, pitch-up, due to the flow separation on the outboard wing panel, did not occur until about 18˚ angle of attack. Neither the original *Aero2s* nor the pitch-up estimation method (which is tied to the baseline method) predict the pitching moment characteristics well. Note that the sweep angles of this configuration differ little from the F-16XL planform.

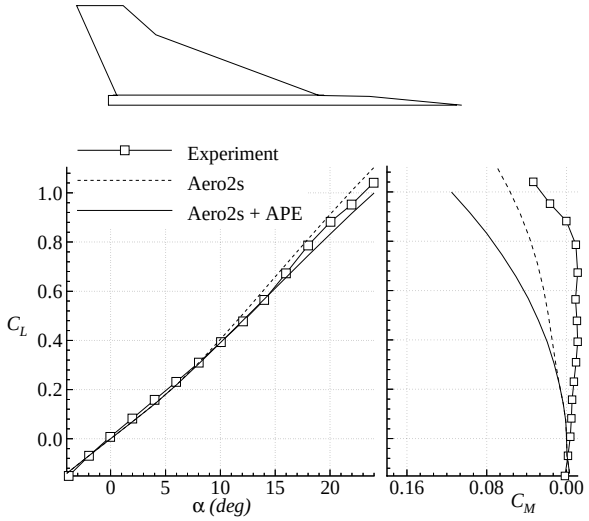

Figure 24. - Comparison of lift and pitching moment estimation methods for a 70˚/48.8˚ sweep uncambered and untwisted cranked arrow wing. Estimates made before “limited vortex” modification.

Here again, if the vortex placement is “limited” for this case, an improvement in the results is found, as shown in Fig. 25. The location of the pitch-up estimation is indicated by the location at which the two curves representing the limited vortex case diverge. This is also close to where there is an initial inflection in the experimental curve. The method fails to estimate the second, and much larger, pitch-up at 20˚ angle of attack.

Note: All subsequent analysis results incorporate the limited vortex modification.

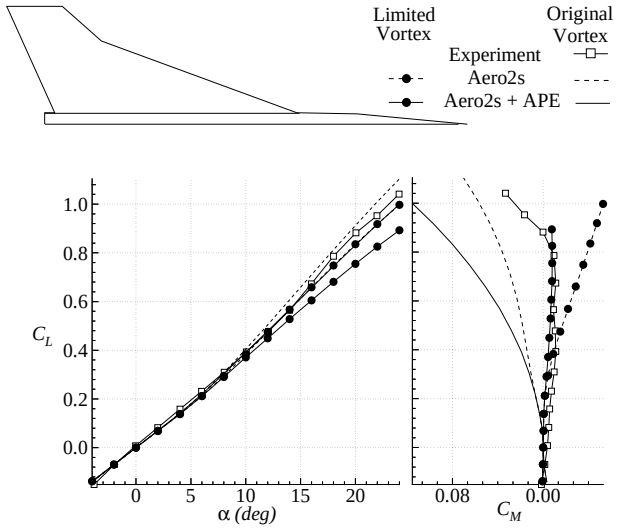

Figure 25. - Effects of limiting the vortex effects to the wing only for a 70˚/48.8˚ sweep uncambered and untwisted cranked arrow wing. Limited vortex begins at wing root and does not to extend into fuselage region.

4.2.2 Horizontal Tail and Flap Effect Analysis

An analysis of the McDonnell Douglas 71˚/57˚ sweep configuration, shown in Fig. 17, was conducted for the configuration with flaps deflected (δ_{TE} = 30˚, δ_{Tail} = 0.0˚, δ_{LE} = 13˚/34˚/35˚/35˚/19˚/29˚). A comparison between the new method and experiment is shown in Fig. 26. A maximum lift coefficient of 1.80 was used for the outboard flapped wing section. The APE method estimate for the lift agrees well throughout the angle of attack range. The estimate of the pitching moment agrees well with the experimental data after the pitch-up, but does not accurately estimate $\partial C_M/\partial C_L$ before the pitch-up. At zero degrees angle of attack, the average slope of the experimentally derived pitching moment curve, $\partial C_M/\partial C_L$, is equal to -0.0855. The corresponding, estimated value for this slope is 0.0623. If the horizontal tail is removed, as shown in Fig. 27, the experimental and estimated values of $\partial C_M/\partial C_L$ are -0.0085 and 0.08688, respectively. The improvement of the estimation suggests the indication of the code's lack of accuracy when predicting the characteristics for the second surface in the presence of the wing wake. The estimation of $\partial C_M/\partial C_L$ for two surface aircraft was shown to improve as the distance between the two surfaces was decreased[29].

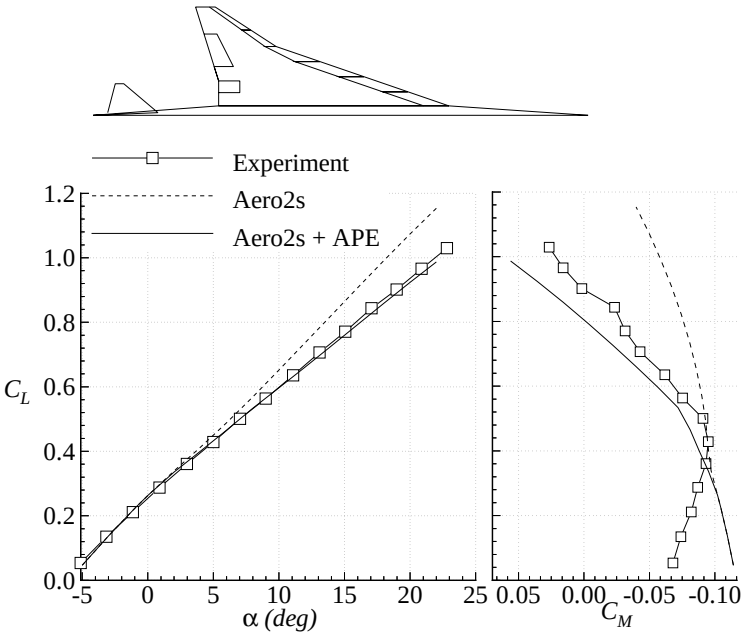

Figure 26. - Comparison of lift and pitching moment estimation methods for a 71˚/57˚ sweep cambered and twisted cranked arrow wing with flaps deflected (δ_{Tail} = 0˚, δ_{TE} = 30˚, δ_{LE} = 13˚/34˚/35˚/35˚/19˚/29˚).

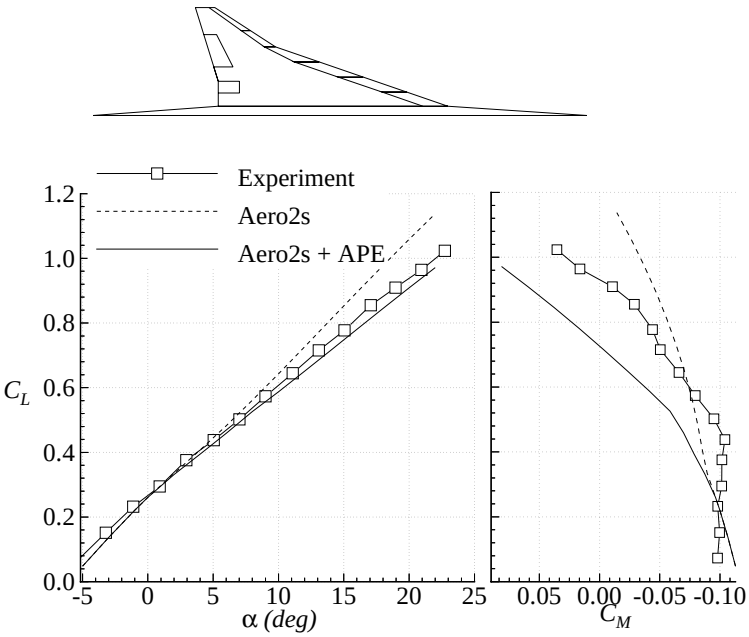

Figure 27. - Comparison of lift and pitching moment estimation methods for a 71˚/57˚ sweep cambered and twisted cranked arrow wing with flaps deflected and tail removed (δ_{TE} = 30˚, δ_{LE} = 13˚/34˚/35˚/35˚/19˚/29˚).

The estimation of the slope of the pitching moment at low angles of attack improved when the flaps were retracted as shown in Fig. 17. This was also true for the same configuration, flaps retracted, with the tail removed, as shown in Fig. 28. Furthermore, the slope of this curve is well predicted for all cases, at higher angles of attack, after the pitch break. It is in this higher angle of attack region that this work is focused.

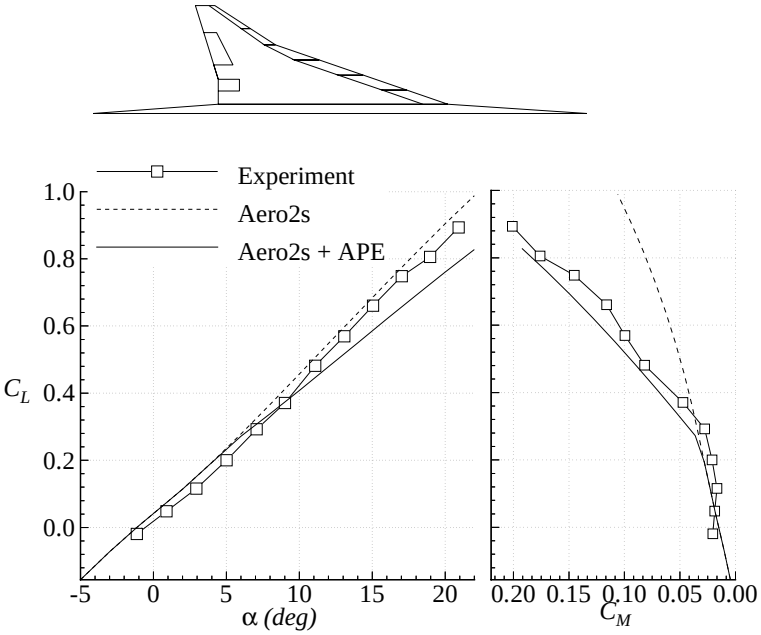

Figure 28. - Comparison of lift and pitching moment estimation methods for a 71˚/57˚ sweep cambered and twisted cranked arrow wing without flaps and horizontal tail removed.

Although the low angle of attack $\partial C_M/\partial C_L$ is not well predicted, the estimated effects of tail deflection correlate well with the experimental data. Figure 29 shows the experimental and theoretically estimated data for the 71˚/57˚ configuration with flaps deflected and tail deflected -10˚. The correlation between the data is similar to that found in Fig. 26 for a zero degrees tail deflection, thus indicating a good prediction of the tail effectiveness (the difference in aerodynamic characteristics between 0˚ and -10˚ tail deflection).

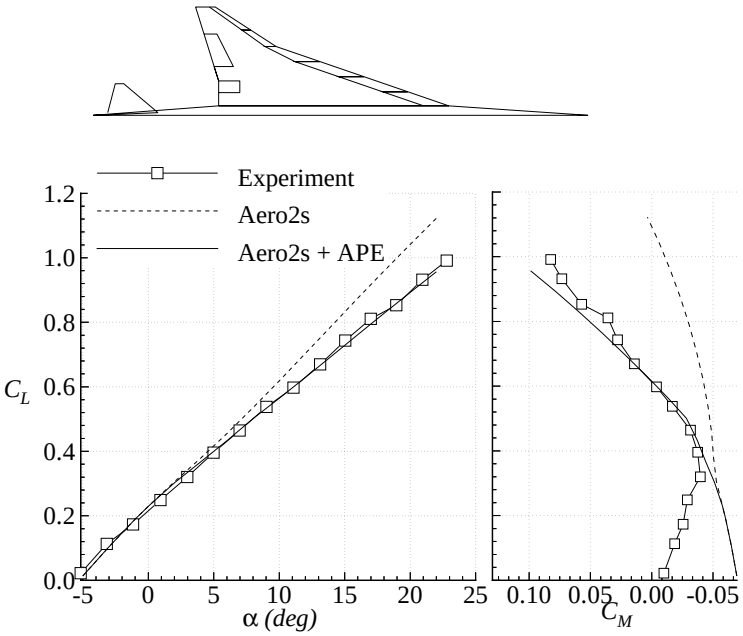

Figure 29. - Comparison of lift and pitching moment estimation methods for a 71˚/57˚ sweep cambered and twisted cranked arrow wing with flaps deflected (δ_{Tail} = -10˚, δ_{TE} = 30˚, δ_{LE} = 13˚/34˚/35˚/35˚/19˚/29˚).

The F-16 XL configuration presented in Fig. 19 is presented again in Fig. 30 for a flaps deflected case. Inboard trailing edge flaps are deflected 30˚, and leading edge flaps are deflected 28˚/38˚/40˚/20˚. A maximum lift coefficient of 1.50 was used. The APE method estimates both the lift and pitching moment well throughout the lift range, although lift is under predicted beginning at about 20˚ angle of attack. The lift coefficient for pitch-up is estimated to occur earlier than when it actually occurs, as opposed to the flaps undeflected case where pitch-up was estimated to occur at a higher C_L than the actual value. The results also indicate an error in the estimation of zero lift pitching moment as was previously found.

The flat wing 74˚/48˚ sweep configuration tested by Kjerstad is presented in Fig. 31 for a 15˚ trailing edge flap deflected case. A maximum lift coefficient of 1.40 was used for this case. The APE method estimated the pitching moment characteristics well, but both the baseline *Aero2s* and the APE method fail to accurately estimate the lift coefficient after about 5˚ angle of attack.

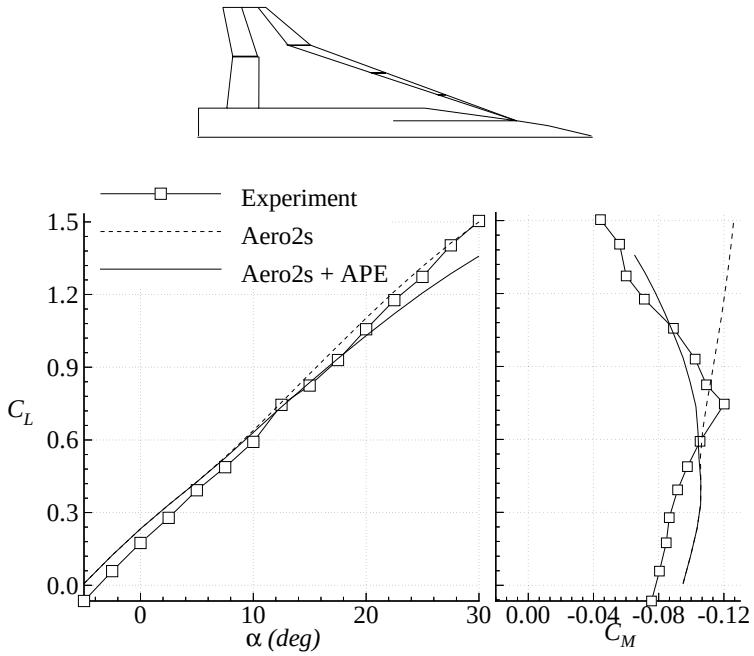

Figure 30. - Comparison of estimation methods for an F-16XL (70˚/50˚ sweep) model test (δ_{LE} = 28˚/38˚/40˚/20˚, δ_{TE} = 30˚/0˚).

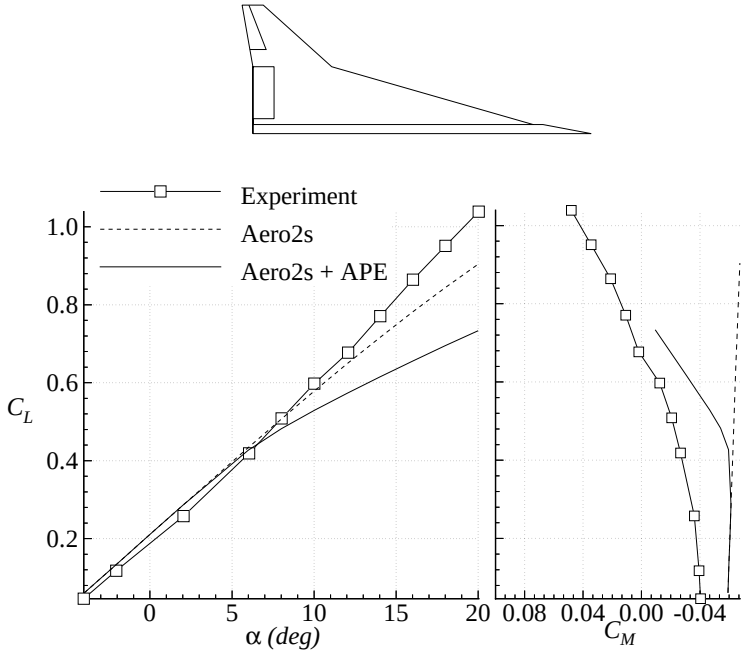

Figure 31. - 74˚/48˚ sweep wing-body combination with trailing edge flaps deflected (δ_{TE} = 15˚).

The AST-200 configuration tested by Coe[11] is presented for a flaps deflected case in Fig. 32. Leading and trailing edge flaps are deflected to 30˚. A maximum 2-D airfoil lift coefficient of 1.50 was chosen for the pitch-up estimation. Results for this case show good agreement between the APE method and experimental results. The lift coefficient at which pitch-up occurs is accurately predicted although the slope of the pitching moment curve after the break is slightly over predicted but within reasonable limits. Note that the pitching moment characteristics are not well predicted by the estimation method for the negative angle of attack range. This result is due to the fact that there is no flow separation limit for negative angles of attack.

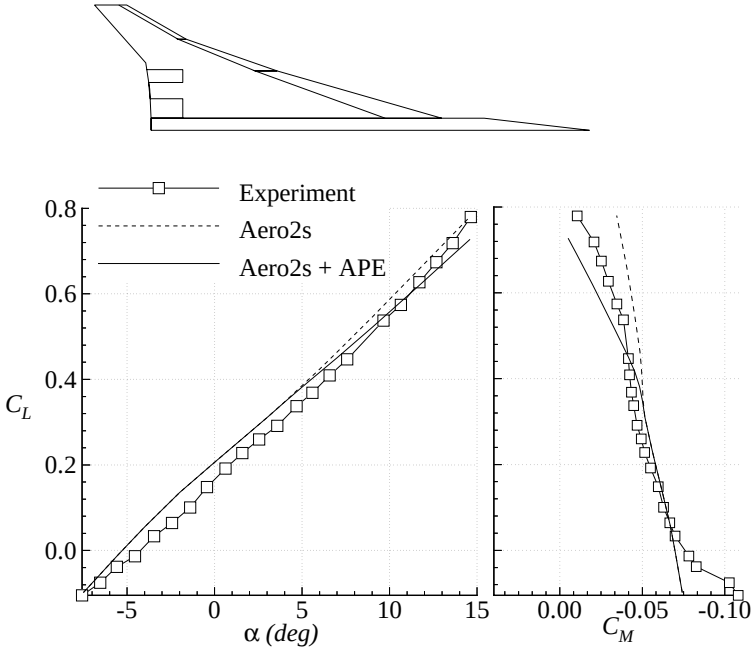

Figure 32. - Comparison of lift and pitching moment estimation methods for a 74˚/70.5˚/60˚ sweep uncambered and untwisted cranked arrow wing similar in planform to the AST-200 with leading and trailing edge flaps deflected (δ_{LE} = 30˚, δ_{TE} = 30˚).

The 70˚/50˚ sweep configuration tested by Quinto and Paulson[51] is shown in Fig. 33 for the configuration with leading edge flaps deflected to 20˚, trailing edge flaps deflected to 30˚, and a maximum 2-D sectional lift coefficient of 1.80. The APE method results for this case are similar to those found for the flaps undeflected case shown in Fig. 25. The pitching moment characteristics are predicted accurately up to an angle of attack of about

18˚ where the pitch-up occurs. This pitch-up is not estimated by the APE method as was the case for the flaps undeflected case. The lift is also under-predicted beginning at about 5˚ angle of attack.

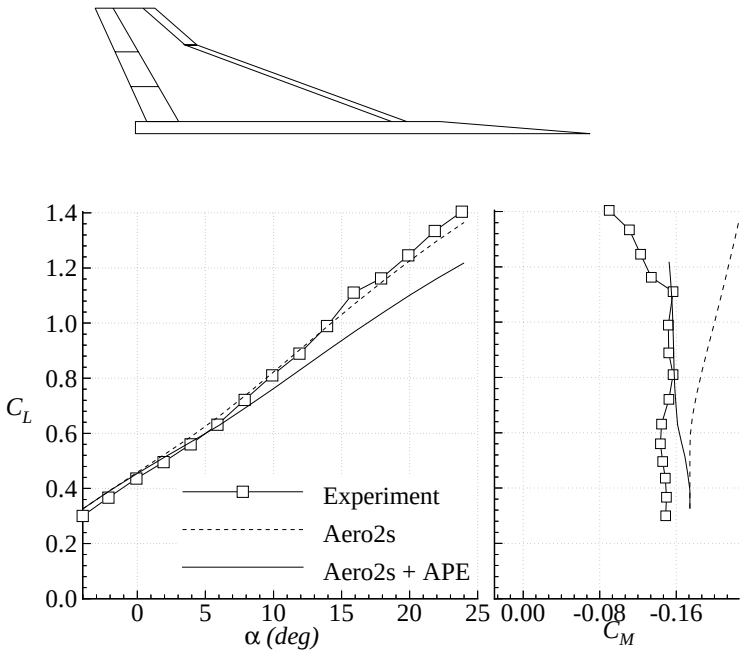

Figure 33. - Comparison of lift and pitching moment estimation methods for a 70˚/48.8˚ sweep uncambered and untwisted cranked arrow wing with flaps deflected (δ_{LE} = 20˚, δ_{TE} = 30˚).

4.3 Method Limitations

A limitation of this method is the inability to distinguish between the effects of small changes to the planform in relation to the effects on the pitching moment. Such effects of changes to the leading edge have already been shown by Grafton. The F-16XL model tested by Hahne incorporated two different leading edges in an effort to model the typical planform of an HSCT configuration, as shown in Fig. 34. Hahne found, as did Grafton, that the small changes in the leading edge shape can drastically affect the pitching moment (Fig. 35). The implication is that although the code predicted the pitching moment characteristics of the F-16XL HSCT configuration well, it would be difficult to account for the changes in flow patterns due to the apex modifications of the baseline configuration.

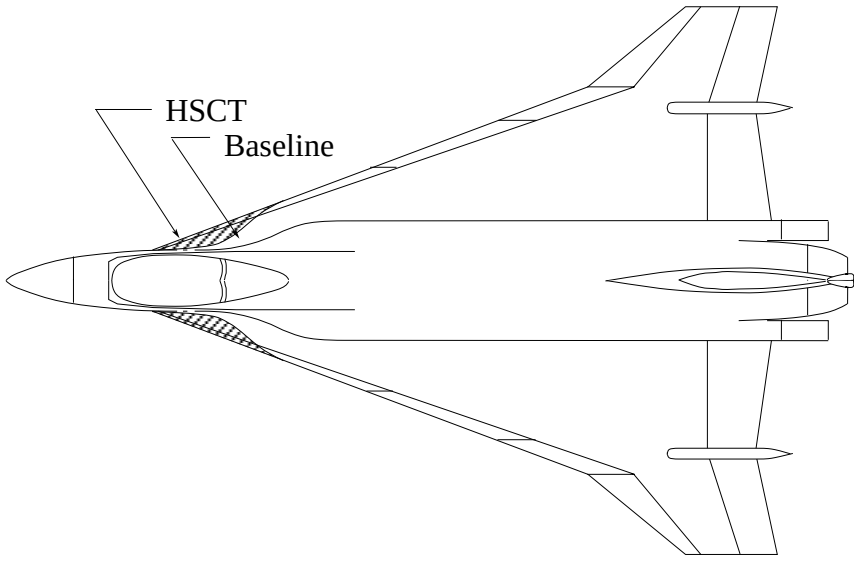

Figure 34. - F-16XL model shown with baseline and HSCT planform configurations.

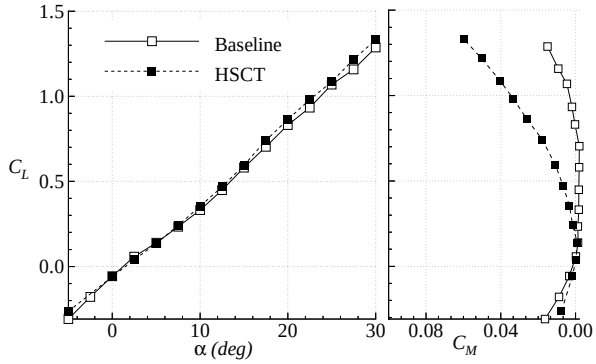

Figure 35. - Effects of apex modifications to the F-16XL aerodynamic characteristics (data taken from an unpublished test).

Another difficulty of the APE method is that maximum airfoil lift coefficients must be prescribed beforehand for the airfoil used. This data requirement includes maximum lift coefficients for leading and trailing edge flap deflections. A typical plot of experimental 2-D airfoil lift and pitching moment data is shown in Fig. 36 for an NACA 63-006 airfoil section.[59] Note that data for only one flap condition is available. An engineering estimate must be made for the maximum lift coefficient if the airfoil used on the outboard wing section is different from what experimental data is available. It would be advantageous to

develop a routine to calculate the maximum lift coefficient as a function of the airfoil geometry definition, Mach number and Reynolds number. Fortunately, good results can be obtained with the APE method with an adequate approximation of the maximum two-dimensional airfoil lift coefficient.

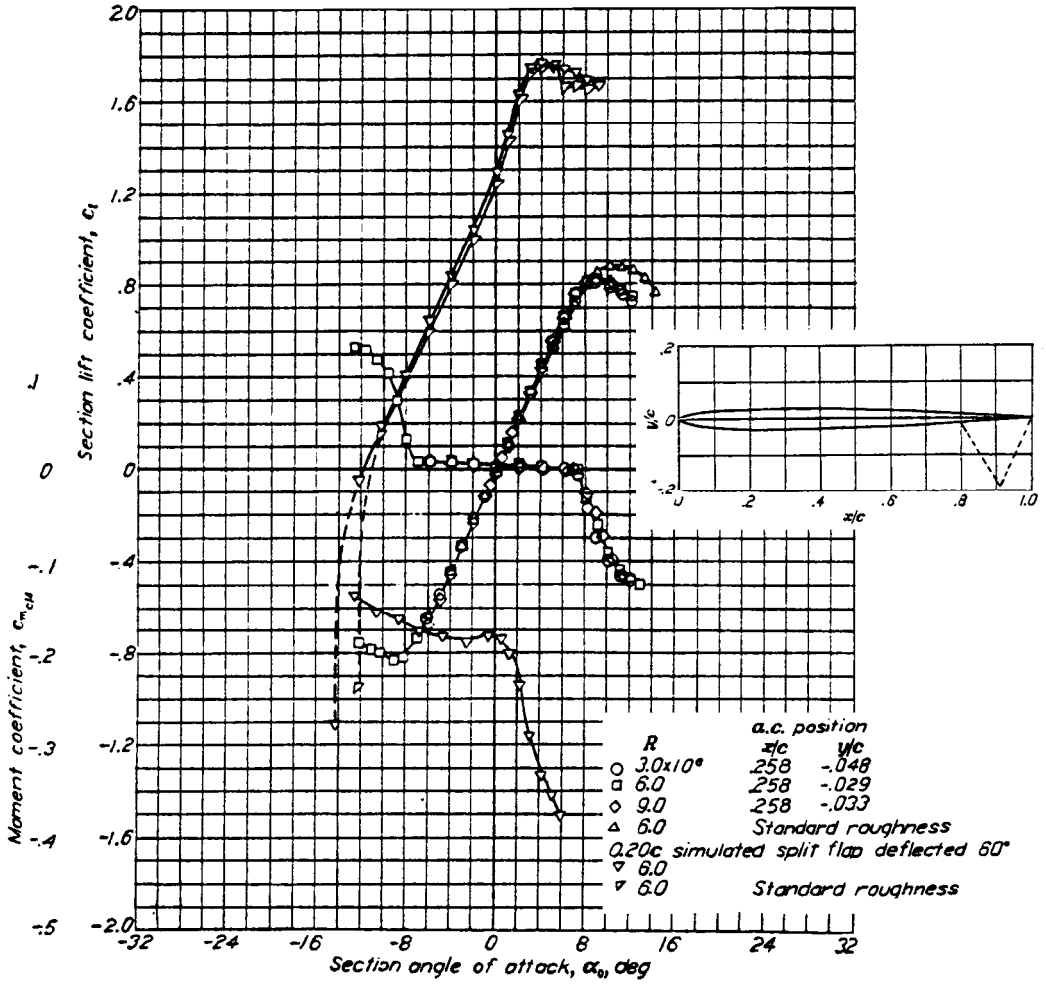

Figure 36. - Two-dimensional airfoil aerodynamic characteristics for an NACA 63-006 airfoil section (ref. 59)

Finally, the APE method does not account for vortex burst or loss of influence. Brandt[60] has proposed a method to estimate vortex burst by modeling the vortex with a derivation of the incompressible Navier-Stokes equations. Brandt has applied this method to a vortex lattice method to estimate the aerodynamic characteristics of highly swept wings at high angles of attack. Analysis of 60˚ and 65˚ delta and arrow wings showed good

correlation between experimental and theoretical results for lift and pitching moment.

The advantage of the APE method is that it does not rely on statistical data correlation to estimate the non-linear aerodynamics of cranked arrow wings, such as the methods used by *DATCOM*, and also provides an estimate of the lift at which pitch-up begins. Although approximate, this method affords a means for making low cost estimates of the aerodynamic characteristics of a cranked arrow wing configuration under consideration for design.

5. Tail/Tailless/Canard Configurations

It was shown in the previous chapter that the deflection of trailing edge flaps creates a negative pitching moment. To trim this moment at low speeds other control surfaces must be deflected or center of gravity control must be employed. For tailless configurations, the center of gravity is placed, and/or moved by means of fuel transfer, such that the configuration is trimmed at a specific lift coefficient. The leading and trailing edge flap systems are scheduled for specific flight speeds so that the required trim lift coefficient is achieved.

Tailless configurations are deemed advantageous because of their decreased weight and drag due to the absence of a canard or horizontal tail.[61] Pitch, high lift, and roll control is shared between control surfaces on these configurations. This configuration limits the control power allocation of each surface and the high lift capability of the aircraft. The limits can create problems at high angles of attack, in the pitch-up region, where adequate pitch-down control is required. Therefore, the use of trailing edge flaps for high lift is often limited. As already discussed, the Concorde relies on vortex lift for adequate landing lift. Current HSCT designs can not afford the resulting noise penalties due to the higher thrust required to overcome the high drag associated with vortex lift. Current HSCT designs must rely on efficient high lift systems for takeoff and landing.

Efficient high lift systems used for takeoff and landing are directly related to the economics of the aircraft operation. Wimpress[62] showed that a five percent increase in the maximum lift could result in a twenty percent increase in payload capability of a transport aircraft (Fig. 37). This result was true for an aircraft that was limited in weight by the available field length. In the case of the modern HSCT aircraft, the maximum lift is limited by a "tail scrape" angle of attack and induced drag. But the dilemma of trimming the negative pitching moment due to trailing edge flaps still exists. Thus, an additional control surface must be added. This control surface can be either a canard or aft horizontal tail. This discussion is not intended to validate one concept over another, but is intended to present the merits and faults of each configuration. Selection of a final design is dependent on the complete analysis of the aircraft in design and off-design conditions with respect to the weight, range, and cost of the final design.

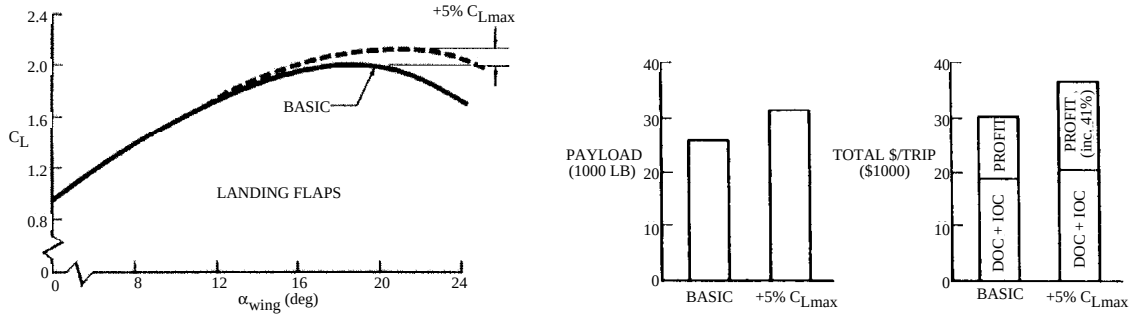

Figure 37. - Economic impact of increasing the maximum lift coefficient of a transport aircraft limited in weight by the available field length (ref. 62).

The low weight and drag of tailless configurations results in lower operating cost and longer range. The poor low speed characteristics, however, can have a considerable effect on the off-design performance. A comparison of the merits of canard versus aft horizontal tail configurations now follows.

Initial impressions of canards make them a favorable choice in configuration design. Canards are generally sized to be about half the size of an aft horizontal tail.[63] For conventional, stable configurations, canards are designed to stall before the wing, thus providing good pitch-down stall characteristics. For fighter configurations, the use of a canard tends to decrease the fuselage length required, compared to the use of an aft horizontal tail.[63] Unfortunately these benefits are not always realized. For highly swept wing configurations the wing does not stall in the same manner as an unswept wing (Fig. 2). A drag rise may be encountered at high angles of attack, but an appreciable loss of lift is not encountered. The problem of pitch-up further complicates the issue. For some unstable configurations, it has been shown that the canard is not as effective in providing pitch-down control as an aft horizontal tail in the high angle of ttack region.[63,64] This is due to the fact that the canard is smaller than an aft horizontal tail and the upwash from the wing increases the local angle of attack of the canard. These results, however, are configuration dependent and may not be true for all configurations. Furthermore, at pitch-up, the canard will actually contribute a positive pitching moment if it is not totally unloaded.[63] Finally, interactions between the canard and fuselage may cause unfavorable effects. Trailing vortices from the canard impinging on the wing cause an increase in the wing lift and can produce either an increase or decrease in the pitching moment. These vortices may also interact with the lateral/ directional control surfaces (ailerons, rudder, etc.) to create

problems in lateral/directional stability and control as shown in Fig. 38.[63,65,66,67] Lateral stability problems with the trailing vortices from the canard impinging on the vertical tail were encountered during the early concept development of the Concorde.[68] These problems in the longitudinal and lateral/directional axes are a function of the canard placement. Experimental investigations have shown that some aircraft, such as a canard configured X-2, do reap the benefits of the higher trimmed lift coefficients and higher lift to drag ratios associated with the use of a canard.[65,69]

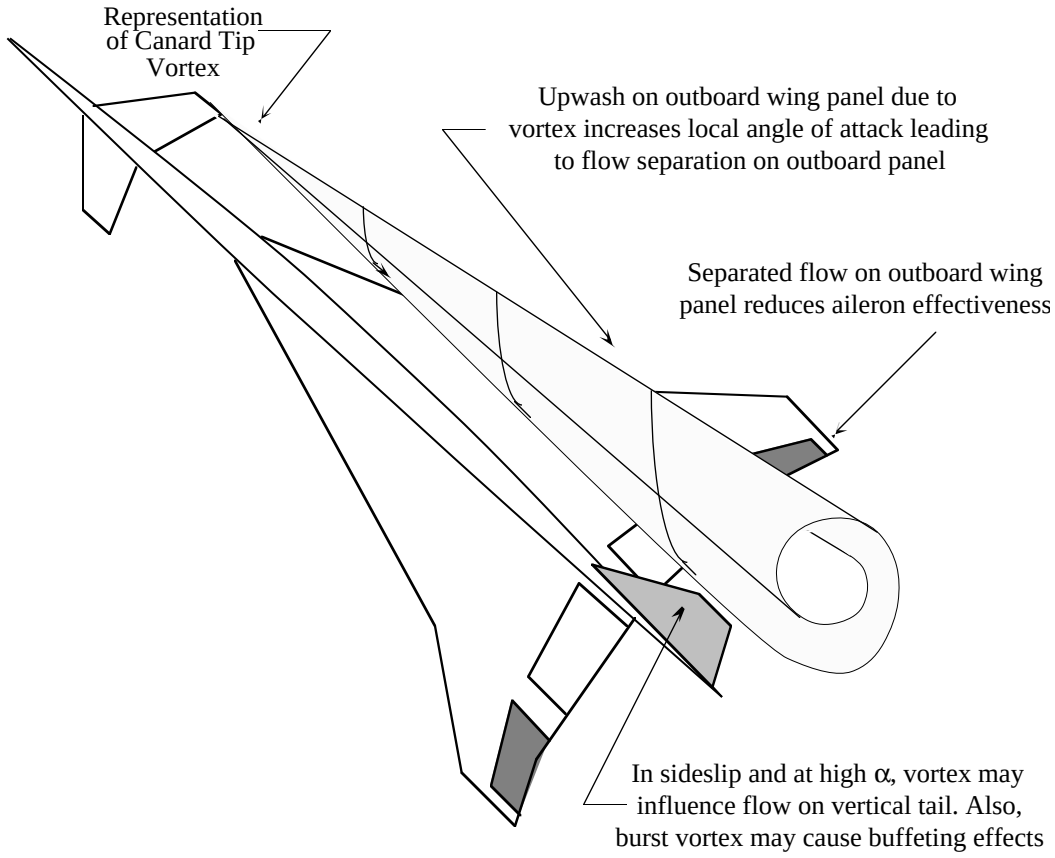

Figure 38. - Effects of canard on lateral/directional stability and control

Aft mounted horizontal tails are not subject to the problem of influencing the wing performance. Rather, the tail is subject to the influence of the wing wake. Fortunately this influence is generally favorable with respect to trimming the aircraft. The downwash from the wing effectively reduces the angle of attack of the local flow on the tail providing for a tail download at small negative tail deflection angles. Pitch-down control is also important,

especially when pitch-up is an issue. However, the effectiveness of the tail, like the canard, is highly dependent on the tail height location of the tail. This relationship is most critical at high angles of attack, where the tail could be rendered ineffective when engulfed in the separated wing wake flowfield.[70,71,72] When this situation occurs, the contribution of the tail to provide pitch-down control is no longer available and the configuration will pitch-up. The tail will regain effectiveness when the aircraft reaches a large enough angle of attack such that the tail is no longer in the wake of the wing. T-tail or high tail arrangements are more susceptible to these problems, thus low mounted tail arrangements would be desirable.

Center of gravity location also plays a role in the performance of a tail/tailless/canard configuration. Center of gravity will not only influence the effectiveness of a particular control surface but dramatically influences the trim drag.[73] It has been shown that canard configurations are more sensitive to center of gravity locations with regard to drag polar shape and pitch control effectiveness.[74] It has also been shown that unstable aircraft benefit from smaller control surface sizes and lower trim drag.[61,74] As stability decreases, the demands on the tail to provide pitch-up control decrease and a smaller tail can be used. For unstable configurations, pitch-down control can be achieved through the deflection of trailing edge flaps and an upload on the aft horizontal tail. The opposite is true for canard configurations. Although, trailing edge flaps are used to provide pitch-down control, a download on the canard is required to provide an additional negative moment, thus reducing the maximum lift. If the tail size is too small, a large load on the surface will be required to trim, increasing the trim drag. Therefore, an optimum tail size and center of gravity location must be chosen to reduce the tail size while minimizing the trim drag and allowing for adequate control power at off-design conditions.

It cannot be over emphasized that the benefits of a horizontal tail/tailless/canard configuration are dependent on the configuration being designed and the operational requirements of the aircraft. The benefits and faults discussed above may be restricted to the planforms studied in the corresponding references. Only comparative studies of the configuration under consideration will reveal which pitch control selection (tail/tailless/canard) will be optimum for the particular flight requirements.

6. Extensions to Multidisciplinary Design Optimization Methodology for HSCT Configurations

The new estimation method was applied to the analysis of a configuration developed during a multidisciplinary design optimization (MDO) program. This program is being conducted at Virginia Tech to generate HSCT configurations that have been optimized to minimize the takeoff gross weight while meeting a variety of design constraints. The interested reader should reference Hutchison.[75,76,77] The starting point of the optimization process is a baseline design shown in Fig. 39. The leading edge sweep angles of this design are 75˚/52˚. An optimized design is also shown in Fig. 39 with leading edge sweep angles of 73.5˚/12˚. A comparison of the aerodynamic characteristics of these two configurations is shown in Fig. 40. The original *Aero2s* method estimate is shown for the optimized configuration only, along with the estimates using *Aero2s* + APE, and is intended to show the difference between current linear methods and the new estimation method. The estimate of the aerodynamic characteristics of the baseline configuration were performed with the APE method. The large sweep angle of the outboard wing section on the baseline configuration resulted in an estimate of a relatively severe pitch-up along with considerably low high angle of attack lift. It should be noted that the APE method is more likely to under-predict the lift for this type of highly swept configuration. Furthermore, the center of gravity position of the optimized configuration, located 175 ft. aft of the nose, was chosen to be about 10% unstable (i.e. $\partial C_M/\partial C_L = 0.106$) after the pitch-up. It was felt that although this number leads to an unstable configuration, it could be controlled with current control systems. The stability level of the baseline configuration is 4.4% stable before the pitch-up and 12.2% unstable after the pitch-up for a center of gravity location of 165 ft. aft of the nose. The effects of choosing a stable center of gravity position for the optimized configuration will be discussed later.

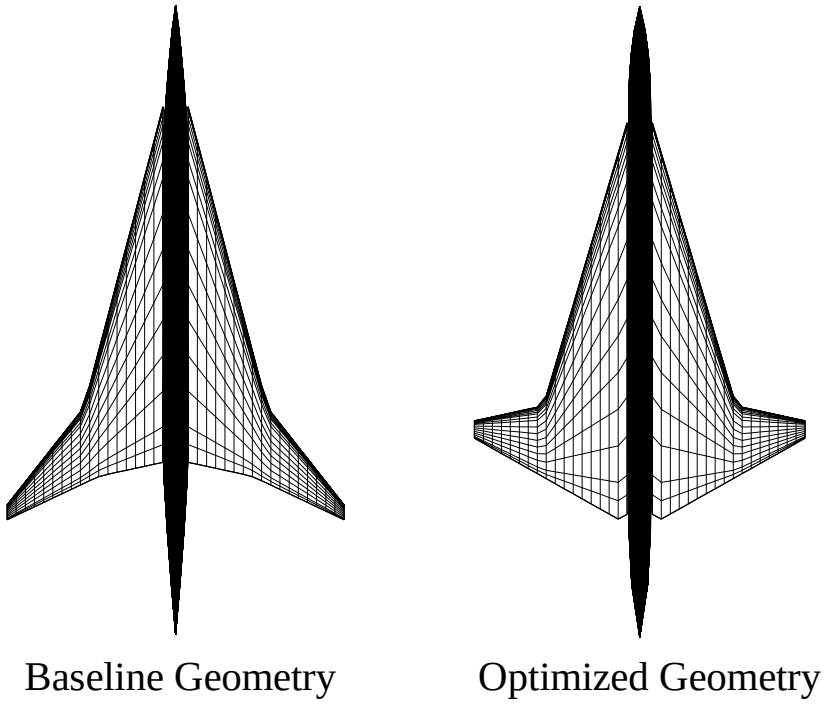

Figure 39. - Configurations developed during a multidisciplinary design optimization program.

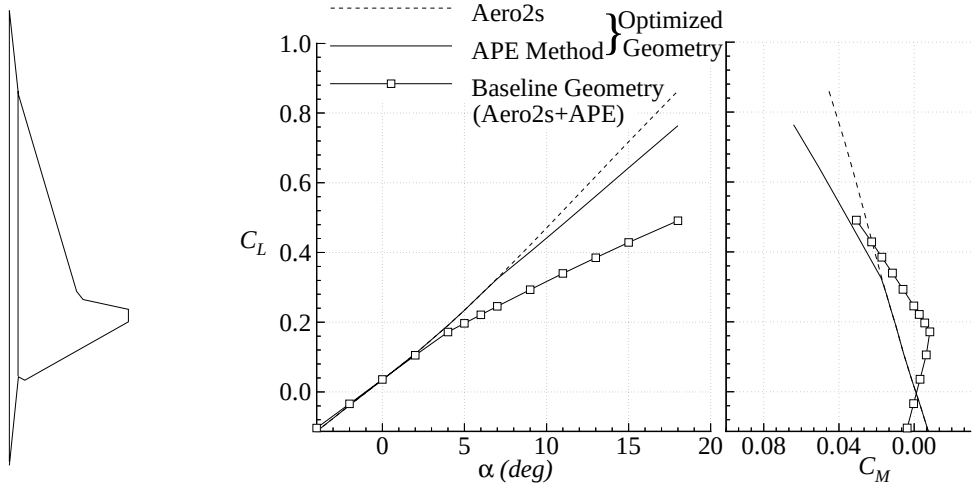

Figure 40. - Aerodynamic characteristics of the baseline and optimized planforms.

Unlike the baseline configuration, the optimized configuration has a very low sweep outboard wing section. During the optimization, it was theorized that this low sweep outboard wing section was due to the maximum 12˚ "tail scrape" landing angle of attack constraint. It has been shown that a reduction of the maximum landing angle of attack to 11˚ resulted in a 4.6% weight penalty.[74] In an effort to reduce the dependence on this constraint and reduce the final configuration weight, trailing edge flaps were added to the configuration with the intent of increasing the low-speed lift. The flap size was chosen to have a root chord equal to 12% of the wing root chord and extend to 40% of the semi-span. The flap was designed such that the hinge line was parallel to the y-axis (i.e. the hinge line was not swept). The flap design was chosen arbitrarily with some attention to designing a flap that was simple and could be feasibly constructed. The APE method estimates for this configuration with the trailing edge flaps is shown in Fig. 41.

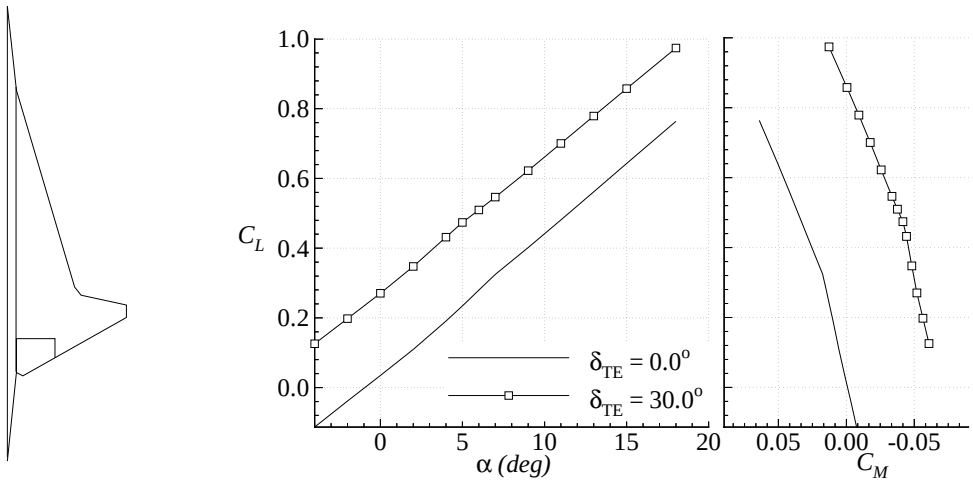

Figure 41. - Effects of adding a trailing edge flap (δ_{TE} = 30˚) to the optimized planform. Analysis performed with the APE method.

As has been previously shown, the deflection of the trailing edge flap creates a negative pitching moment which must be trimmed for level flight. Therefore, a horizontal tail was added to the configuration for the purpose of trimming the aircraft at the required landing lift coefficient. The landing lift coefficient, C_L, is determined from the landing weight of the aircraft, landing speed, wing area, and air density. This value will obviously be different for each configuration, therefore an average value of 0.60 was chosen. This value is close to the actual required C_L for the configurations that have been generated in

the past by the MDO program. Fig. 41 indicates that the optimized configuration achieved the 0.60 lift coefficient at about $\alpha = 14^{\circ}$. The APE method was shown to estimate lower lift coefficients than the aerodynamic analysis used in the MDO program which calculated a landing angle of attack equal to 12˚. The tail design was similar to those used for previously designed supersonic transports. The tail was sized for an area equal to 6.22% of the wing area with a leading edge sweep of 46.6˚. This size is typical for supersonic transport type aircraft. For example, the tail area of the McDonnell Douglas AST configuration is equal to 7.75% of the wing area.

Results of the configuration with the horizontal tail and trailing edge flaps deflected using the APE method are shown in Fig. 42. The horizontal tail was deflected -5˚ to trim the aircraft at about $C_L = 0.60$. Included in the figure are the results for the flap deflected and flap undeflected cases without the horizontal tail for comparison. Note that the addition of the horizontal tail for trim results in a loss of lift compared to the no-tail, flap deflected condition. However, the addition of the horizontal tail and trailing edge flaps results in a significant increase in the low speed lift compared to the original configuration. This translates into a reduction of landing angle of attack by 4.6˚ or an increase in lift coefficient of 0.185 at $\alpha = 9.3^{\circ}$.

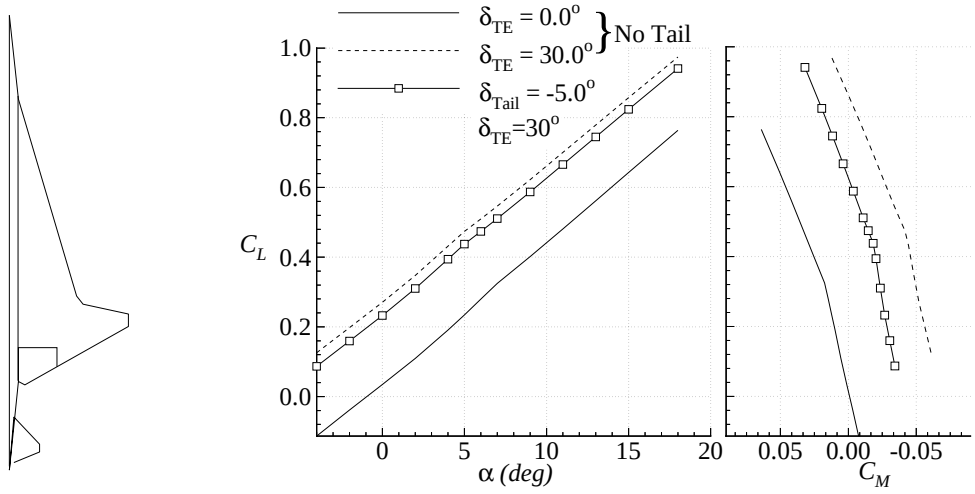

Figure 42. - Aerodynamic performance of a trailing edge flap and horizontal tail combination ($\delta_{Tail} = -5^{\circ}$, $\delta_{TE} = 30^{\circ}$) calculated with the APE method.

The original optimized configuration shown in Fig. 42 is not trimmed at the prescribed landing lift coefficient. For this to occur the trailing edge would have to be

deflected, which would also increase the lift, or the center of gravity would have to be changed, by means of fuel transfer. To trim at the prescribed center of gravity location the trailing edge would have to be deflected 18˚. The resulting increased lift, as shown in Fig. 43, would reduce the landing angle of attack by 3.5˚. The increase in lift at the trimmed angle of attack of 11˚ is 0.143. Thus the effects of trimming the original optimized tailless configuration results in an increase in landing lift not previously accounted for during the optimization process. However, for a tailless configuration the trailing edge flap would be required to deflect up and down, thus a plain flap would have to be used. For such a flap design, a 30˚ deflection angle would be considered to be a maximum effective deflection angle. Fig. 42 shows that a 30˚ deflection angle for the tailless configuration would not provide any pitch-down control above 16˚ angle of attack. For this tailless configuration to be a viable design, additional pitch-control surfaces would have to be added. Had this analysis been performed without the APE method, a different result would be attained as shown in Fig. 44. Note that the flap deflection angle to trim was determined to be only 13˚ and that pitch-down control is available beyond 20˚ angle of attack. This result shows the impact and benefits of using the APE method during the preliminary phase. This analysis has set the stage for a trade-off study between the aft tail and tailless configurations.

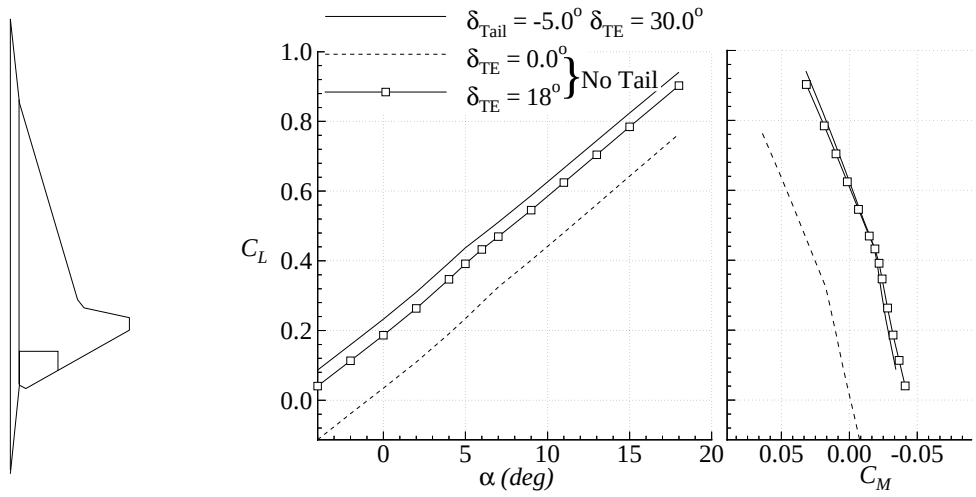

Figure 43. - Comparison of the trimmed tail and tailless configurations calculated with the APE method.

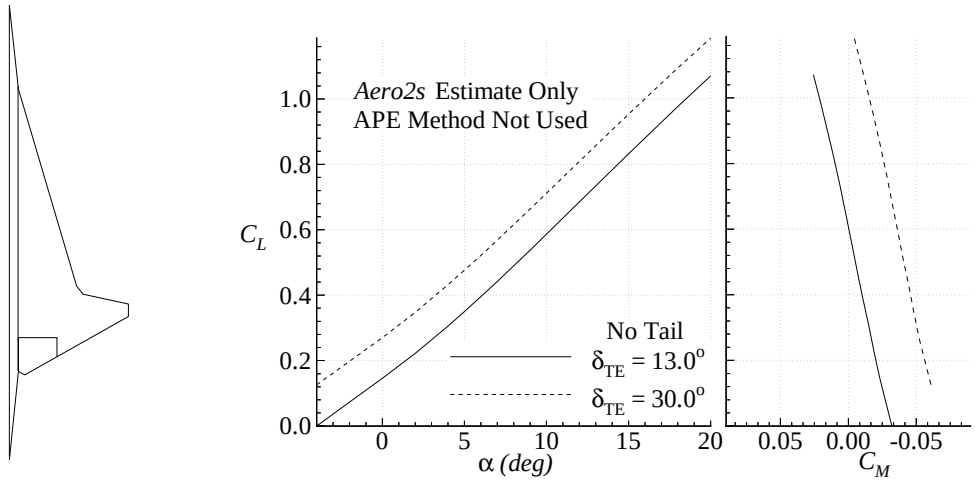

Figure 44. - Analysis of the tailless configuration without the APE method.

For the configurations described above a center of gravity position of 175 ft aft of the nose was chosen to give the unstable characteristics. An example was shown of how to trim the tailless configuration with only the trailing edge flaps. If center of gravity control were used to trim at the landing lift coefficient, the center of gravity would have to be moved forward by 10 ft (7.65% of the mean aerodynamic chord). Obviously no change in the low-speed lift would be attained by simply moving the center of gravity. If the trailing edge flaps were deflected to 30˚ to increase the low-speed lift, a tail deflection of -27.5˚ would be required to trim. For this center of gravity position the benefits of using flaps and a horizontal tail are reduced, as shown in a comparison to the 175 ft center of gravity position in Fig. 45. The forward center of gravity position with tail and flap deflection results in a reduction in the lift coefficient equal to 0.069 compared to the case of the flaps and tail deflected and the center of gravity at 175 ft. The lift coefficient for this case was also 0.027 less than the case of the tailless configuration with flaps deflected 18˚ and center of gravity at 175 ft. However, the low speed lift coefficient for this case was superior to the original tailless configuration without flaps with an increase in lift coefficient equal to 0.116. Although the forward center of gravity position allows for stable pitching moment characteristics, the benefits of using a high lift system is reduced. Also, it is likely that the horizontal tail will not be effective at a deflection angle equal to -27.5˚ suggesting that a larger tail would be required to trim.

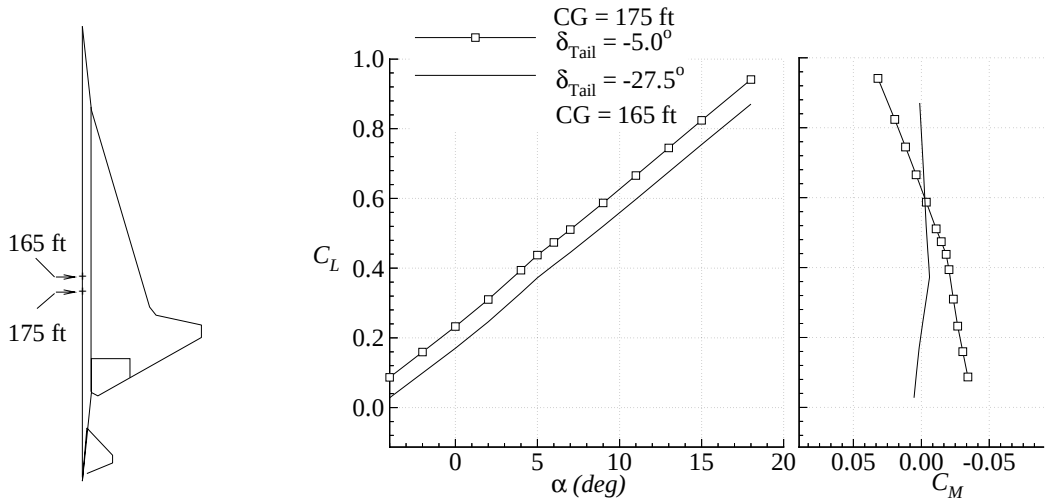

Figure 45. - Effects of changing the center of gravity location for a configuration (δ_{TE} = 30˚) on the trimmed lift coefficient. Results for initial flap deflected case (δ_{Tail} = -5˚) were computed with a center of gravity position equal to 175 ft aft of the nose.

The above analysis was for the purpose of exploring and demonstrating the effects of trailing edge flap devices and horizontal tail on the trimmed lift coefficient. Although, the APE method is likely to under-predict the lift in many cases, the relative change in the lift due to the deflection of these devices should be unaffected by the under-prediction of lift. It should also be noted that these configurations, to be efficient at low speeds, will likely incorporate leading edge flap devices with the intent of reducing the vortex lift and thus the associated drag. This consideration should be taken into account in the multidisciplinary design optimization program which currently assumes that landing lift will include full vortex lift. A summary of the effects of incorporating trailing edge flaps in the aerodynamic analysis of a preliminary design is shown in Table 1 for an unstable and a stable center of gravity position.

6.1 Application to Multidisciplinary Design Optimization Process

The preceding analysis simply added an arbitrary flap and horizontal tail to improve the low-speed characteristics. By doing so, the low-speed aerodynamic characteristics were improved but the design of the configuration is no longer optimum. That is, the optimization was conducted such that the design met the 12˚ tail scrape angle. With the addition of flaps, the landing angle was reduced and it is possible that a more efficient

design could be obtained with the increase in lift and reduced dependence on meeting the tail scrape angle. One means of accounting for this would be to include flap and tail design routines in the MDO program, along with a thorough subsonic aerodynamic analysis which would include the calculation of the trimmed lift and drag coefficients. This approach might lead to a better design but it would be computationally costly. A simpler approach would be to examine the results above and estimate the amount of additional lift that could be achieved with the use of trailing edge flaps. An estimate of the center of gravity range would be required to make a proper estimate of the lift increment. The optimization could then be rerun with the prescribed reduction in landing lift. If it is decided that a horizontal tail is required to trim, the additional weight and drag of this surface should be included in the optimization. With this approach the APE method would be used for analysis of the final design to determine if the low-speed requirements are actually met.

To increase the complexity of the optimization, the APE method could be used in each design cycle as described above. To reduce the computational cost of this approach, it could be implemented only when the optimizer has reached a solution close to an optimum. The complexity of the design could also include optimizing flap and tail size for minimum weight and drag. Finally, a leading edge flap system should be designed to minimize the vortex lift and thus the low-speed drag. The reduction of the low-speed drag is important in meeting the takeoff and landing noise requirements.

Table 1. - Summary of flap effects on the optimized configuration

Configuration	Flap / Tail Deflection	CG (aft of nose)	$\Delta\alpha$ @ Trim C_L	ΔC_L @ Trim α
Tailless	0˚	165 ft. Neutral Stability	0	0
Tail	30˚ / -27.5˚		-2.88˚	0.116
Tailless	18˚	175 ft ~10% Unstable	-3.56˚	0.143
Tail	30˚ / -5˚		-4.61˚	0.185

7. Conclusions & Recommendations

Many current configurations developed for supersonic transport aircraft are prone to the problem of an unstable pitch-up at angles of attack well within the low speed operating regime. It is important for the configuration designer to be aware of the aerodynamic reasons for pitch-up and the geometric factors that contribute to pitch-up and affect the type of the pitch-up behavior. Several key findings were identified and presented in this research. They are:

- The mechanism by which pitch-up occurs. Two prime causes for pitch-up were identified. These were: 1) classical flow separation on the outboard wing section, and 2) the dominating influence of an inboard leading edge vortex coupled with vortex bursting at the trailing edge.
- Geometric factors which affect the pitch-up behavior, including planform shape and control surface deflection.
- Previously investigated methods to postpone the pitch-up behavior and improve longitudinal aerodynamics of cranked arrow wings.
- The effectiveness of flaps on highly-swept, low aspect ratio configurations.
- The development of a new method to estimate pitch-up and validation of this method with experimental data.
- Application of the new method to preliminary aircraft design

The new method resulted in a simple and computationally inexpensive means of estimating the onset of non-linear aerodynamic characteristics and pitch-up of cranked arrow wings, as shown through numerous comparisons with data. The method was especially effective in estimating pitch-up when the occurrence was due to classical flow separation on the outboard wing panel.

Refinement of the APE method should include the improvement of the high angle of attack lift and drag predictions. A method to calculate the maximum lift coefficient of a particular airfoil would also improve the operation of the method. The calculation of the maximum lift of the airfoil could be related to Carlson's attainable thrust method. The maximum lift coefficient could be calculated from empirical data for the maximum angle of attack for attached flow on an airfoil based on the airfoil geometry, Reynolds number and Mach number. Furthermore, a routine to calculate the trimmed lift and drag

coefficients would also be helpful in the application of this method to aircraft design. This routine should include flap and tail contributions. Finally, to increase the complexity of the design approach, flap and tail design variables should be included in the MDO process to design an efficient high lift system.

References

1. Wright, B.R., F. Bruckman, and N.A. Radovich, “Arrow Wings for Supersonic Cruise Aircraft,” *Journal of Aircraft*, Vol. 15, No. 12, pp. 829-836, December 3, 1978.

2. Nelson, C.P. “Effects of Wing Planform On HSCT Off-Design Aerodynamics,” AIAA-92-2629-CP, 1992.

3. Spearman, Leroy M. “The Evolution of the High-Speed Civil Transport,” NASA TM 109089, 1994.

4. Antani, D.L. and J.M. Morgenstern. “HSCT High-Lift Aerodynamic Technology Requirements,” AIAA-92-4228, Aircraft Design Systems Meeting, 1992.

5. Swan, W.C. “Design Evolution of the Boeing 2707-300 Supersonic Transport, Part I - Configuration Development, Aerodynamics, Propulsion, and Structures,” AGARD CP-147, Oct. 1973.

6. Coe, Paul L., Jr., H. Clyde McLemore, and James P. Shivers. "Effects of Upper-Surface Blowing and Thrust Vectoring on Low-Speed Aerodynamic Characteristics of a Large-Scale Supersonic Transport Model," NASA TN D-8296, 1976.

7. Coe, Paul L., Jr., Paul M. Smith, and Lysle P. Parlett. “Low Speed Wind Tunnel Investigation of an Advanced Supersonic Cruise Arrow-Wing Configuration,” NASA TM 74043, 1977.

8. Coe, Paul L., Jr. and Robert P. Weston. “Effects of Wing Leading-Edge Deflection on Low-Speed Aerodynamic Characteristics of a Low-Aspect-Ratio Highly Swept Arrow-Wing Configuration,” NASA TP 1434, 1979.

9. Coe, Paul L., Jr. and James L. Thomas. “Theoretical and Experimental Investigation of Ground-Induced Effects for a Low-Aspect-Ratio Highly Swept Arrow-Wing Configuration,” NASA TP 1508, 1979.

10. Coe, Paul L, Jr., Jarrett K. Huffman, and James W. Fenbert. “Leading-Edge Deflection Optimization for a Highly Swept Arrow-Wing Configuration,” NASA TP 1777, 1980.

11. Coe, Paul L., Scott O. Kjelgaard, and Garl L. Gentry Jr. “Low Speed Aerodynamic Characteristics of a Highly Swept, Untwisted, Uncambered Arrow Wing,” NASA TP 2176, 1983.

12. Freeman, Delma C., Jr. and Richard D'Amato. “The Aerodynamic Characteristics of a Fixed Arrow Wing Supersonic Transport Configuration (SCAT 15F-9898) Part II - Stability Characteristics In the Deep Stall Angle of Attack Range,” NASA LWP-724, 1969.

13. Lockwood, Vernard E. “Effect of Leading Edge Contour and Vertical-Tail Configuration on the Low-Speed Stability Characteristics of a Supersonic Transport Model a Having Highly-Swept Arrow Wing,” NASA TM 78683, 1978.

14. McLemore, H. Clyde, Lysle P. Parlett, and William Sewall. “Low-Speed Wind-Tunnel Tests of 1/9-Scale Model of a Variable-Sweep Supersonic Cruise Aircraft,” NASA TN D-8380, 1977.

15. Radkey, R.L., H.R. Welge, and J.E. Felix. “Aerodynamic Characteristics of a Mach 2.2 Advanced Supersonic Cruise Aircraft Configuration at Mach Numbers from 0.5 to 2.4,” NASA CR 145094, 1977.

16. Re, Richard J. and Lana M. Couch. “The Aerodynamic Characteristics of a Fixed Arrow Wing Supersonic Transport Configuration (SCAT 15F-9898) Part III - Reynolds Number Effects on the Stability Characteristics In the Deep Stall Angle of Attack Range,” NASA LWP-735, 1969.

17. Shivers, James P., H. Clyde McLemore, and Paul L. Coe, Jr. “Low-Speed Wind-Tunnel Investigation of a Large-Scale Advanced Arrow-Wing Supersonic Transport Configuration with Engines Mounted Above Wing for Upper-Surface Blowing,” NASA TN D-8350, 1976.

18. Smith, Paul. “Low-Speed Aerodynamic Characteristics from Wind-Tunnel Tests of a Large-Scale Advanced Arrow-Wing Supersonic Transport Concept,” NASA CR 145280, 1978.

19. Yip, Long P. and Lysle P. Parlett. “Low-Speed Wind-Tunnel Tests of a 1/10-Scale Model of an Arrow-Wing Supersonic Cruise Configuration Designed for Cruise at Mach 2.2,” NASA TM 80152, 1979.

20. Barber, Hal T., Jr. and E.E. Swanson. “Advanced Supersonic Technology Concept AST-100 Characteristics Developed in a Baseline-Update Study,” NASA TM X-72815, 1976.

21. Barber, Hal T. “Characteristics of the Advanced Supersonic Technology AST-105-1 Configured for Transpacific Range with Pratt and Whitney Aircraft Variable Stream Control Engines,” NASA TM 78818, 1979.

22. Barber, Hal T., Jr. “Characteristics of an Advanced Supersonic Technology Transport (AST-106-1) Configured with Variable-Cycle Engines for Transpacific Range,” NASA TM 81879, 1982.

23. Douglas Aircraft Company. “Study of High-Speed Civil Transports,” NASA CR 4236, 1990.

24. Douglas Aircraft Company. “1989 High-Speed Civil Transport Studies,” NASA CR 4375, 1991.

25. Kehrer, W.T. “Design Evolution of the Boeing 2707-300 Supersonic Transport, Part II - Design Impact of Handling Qualities Criteria, Flight Control Systems Concepts, and Aeroelastic Effects on Stability and Control,” AGARD CP-147, Oct. 1973.

26. Robins, A. Warner, Samuel M. Dollyhigh, Fred L. Beissner, Jr., Karl Geiselhart, Glenn L. Martin, E.W. Shields, E.E. Swanson, Peter G. Coen, and Shelby J. Morris, Jr. “Concept Development of a Mach 3.0 High-Speed Civil Transport,” NASA TM 4058, 1988.

27. Walkley, Kenneth B. and Glenn L. Martin. “Aerodynamic Design and Analysis of the AST-200 Supersonic Transport Configuration Concept,” NASA CR 159051, 1979.

28. Walkley, K.B., G.J. Espil, W.A. Lovell, G.L. Martin, and E.E. Swanson. “Concept Development of a Mach 2.7 Advanced Technology Transport Employing Wing-Fuselage Blending,” NASA CR 165739, 1981.

29. Carlson, Harry W., Christine M. Darden, and Michael J. Mann. “Validation of a Computer Code for Analysis of Subsonic Aerodynamic Performance of Wings With Flaps in Combination With a Canard or Horizontal Tail and an Application to Optimization,” NASA TP 2961, 1990.

30. Shortal, Joseph A. and Bernard Maggin. “Effect of Sweepback and Aspect Ratio on Longitudinal Stability Characteristics of Wings at Low Speeds,” NACA TN 1093, 1946.

31. Lamar, John E. “High Angle of Attack - Aerodynamics. AGARD Special Course on Engineering Methods in Aerodynamic Analysis and Design of Aircraft,” AGARD Report 783, 1992.

32. Spreeman, Kenneth P. “Design Guide for Pitch-Up Evaluation and Investigation at High Subsonic Speeds of Possible Limitations Due to Wing-Aspect-Ratio Variations,” NASA TM X-26, 1959.

33. Kulfan, R.M. "Wing Airfoil Shape Effects on the Development of Leading-Edge Vortices," AIAA 79-1675, 1979.

34. Kulfan, R.M. “Wing Geometry Effects on Leading Edge Vortices,” AIAA-79-1872, 1979.

35. Wentz, William H., Jr. *Wind Tunnel Investigations of Vortex Breakdown on Slender Sharp-Edged Wings.* Ph.D. Thesis, University of Kansas, 1968 (also NASA CR 98737 with David L. Kohlman).

36. Rao, Dhanvada M. “Exploratory Investigation of a Tip Blowing Concept on a Cranked-Arrow ‘HSCT’ Planform,” AIAA-92-2637, 1992.

37. Poisson-Quinton, P. “Slender Wings for Civil and Military Aircraft,” Eighth Theodore von Karman Memorial Lecture, *Israel Journal of Technology*, Vol. 16, No. 3, pp. 97-131, 1978.

38. Grafton, Sue B. “Low-Speed Wind-Tunnel Study of the High-Angle-of-Attack Stability and Control Characteristics of a Cranked-Arrow-Wing Fighter Configuration,” NASA TM 85776, 1984.

39. Lamar, John E., Roy T. Schemensky, and C. Subba Reddy. “Development of a Vortex-Lift Design Procedure and Application to a Slender Maneuver-Wing Configuration,” *Journal of Aircraft*, Vol. 18, No. 4, April 1981, pp. 259-266.

40. Hom, K.W., O.A. Morris, and D.E. Hahne. “Low Speed Investigation of the Maneuver Capability of Supersonic Fighter Wings.” AIAA 21st Aerospace Sciences Meeting, January 1983, Reno, Nevada. AIAA-83-0426.

41. Grafton, Sue B. and Luat T. Nguyen. “Wind Tunnel Free Flight Investigation of a Model of a Cranked-Arrow-Wing Fighter Configuration,” NASA TP 2410, 1985

42. Furlong, G. Chester and James G. McHugh. “A Summary and Analysis of the Low-Speed Longitudinal Characteristics of Swept Wings at High Reynolds Number,” NACA Report 1339, 1957.

43. McLemore, H. Clyde and Lysle P. Parlett. “Low-Speed Wind-Tunnel Tests of a 1/10-Scale Model of a Blended-Arrow Supersonic Cruise Aircraft,” NASA TN D-8410, 1977.

44. Malcolm, Gerald N. and Robert C. Nelson. “Comparison of Water and Wind Tunnel Flow Visualization Results on a Generic Fighter Configuration at High Angles of Attack,” AIAA-87-2423, 1987.

45. Mason, W.H. “What We Need in Experimental Aerodynamics: One Engineering Educator’s View (Invited),” AIAA 30th Aerospace Sciences Meeting, January 1992. AIAA-92-0161.

46. Johnson, Joseph L., Jr., Sue B. Grafton, and Long P. Yip. “Exploratory Investigation of the Effects of Vortex Bursting on the High Angle-of-Attack Lateral-Directional Stability Characteristics of Highly-Swept Wings,” AIAA 80-0463, 1980.

47. Rao, Dhanvada M. and Thomas D. Johnson, Jr. “Subsonic Pitch-up Alleviation on a 74 Deg Delta Wing,” NASA CR 165749, 1981.

48. Shevell, R.S. “Aerodynamic Bugs: Can CFD Spray them Away?” AIAA-85-4067, 1985.

49. Bradley, R.G., W.O. Wray, and C.W. Smith. “An Experimental Investigation of Leading-Edge Vortex Augmentation by Blowing,” NASA CR-132415, 1974.

50. Wolowicz, Chester H. and Roxanah B. Yancey. “Summary of Stability and Control Characteristics of the XB-70 Airplane,” NASA TM X-2933, 1973.

51. Quinto, P. Frank and John W. Paulson. “Flap Effectiveness on Subsonic Longitudinal Aerodynamic Characteristics of a Modified Arrow Wing,” NASA TM 84582, 1983.

52. Lamar, John E. and Henry E. Herbert. “Production Version of the Extended NASA-Langley Vortex Lattice FORTRAN Computer Program - Volume I - User's Guide,” NASA TM 83303, 1982.

53. Carlson, Harry W. and Kenneth B. Walkley. “An Aerodynamic Analysis Computer Program and Design Notes for Low Speed Wing Flap Systems,” NASA CR 3675, 1983.

54. Lamar, John E. and Blair B. Gloss. “Subsonic Aerodynamic Characteristics of Interacting Lifting Surfaces with Separated Flow Around Sharp Edges Predicted by a Vortex Lattice Method,” NASA TN D-7921, 1975.

55. Lamar, John, E. “Extension of Leading-Edge Suction Analogy to Wings with Separated Flow Around the Side Edges at Subsonic Speeds,” NASA TR-R-428, 1974.

56. Carlson, Harry W., Robert J. Mack, and Raymond L. Barger. “Estimation of Attainable Leading-Edge Thrust for Wings at Subsonic and Supersonic Speeds,” NASA TP 1500, 1979.

57. Carlson, Harry W. and Kenneth B. Walkley. “A Computer Program for Wing Subsonic Aerodynamic Performance Estimates Including Attainable Thrust and Vortex Lift Effects,” NASA CR 3515, 1982.

58. Hoerner, Sighard F. and Henry V. Borst. *Fluid-Dynamic Lift*, Hoerner Fluid Dynamics, Brick Town, New Jersey, 1975.

59. Abbott, Ira A. and Albert E. Von Doenhoff. *Theory of Wing Sections*, Dover Publications, Inc., New York, 1949.

60. Brandt, Steven A. “A Vortex Burst Model for Enhancement of the Vortex Lattice Method at High Angles of Attack,” AIAA 94-0074, 1994.

61. Kroo, Ilan. “Tail Sizing for Fuel-Efficient Transports,” AIAA-83-2476, 1983.

62. Wimpress, J.K. “Aerodynamic Technology Applied to Takeoff and Landing,” *Annals of the New York Academy of Sciences*, Vol. 154, Art. 2, pp. 962-981, November 22, 1968.

63. Wedekind, G. “Tail Versus Canard Configuration An Aerodynamic Comparison with Regard to the Suitability for Future Tactical Combat Aircraft,” ICAS-82-1.2.2, 1982.

64. Fellers, W.E., W.S. Bowman, and P.T. Wooler. “Tail Configurations for Highly Maneuverable Combat Aircraft,” AGARD CP-319, October 1981.

65. Spearman, M. Leroy. “Some Lessons Learned with Wind Tunnels,” AIAA 86-0777, 1986.

66. Mason, W.H., Joe Mazza, Alex Benoliel, and Eric. C. Johnson. “Lockspeiser LDA-1000 Aircraft Evaluation and Test,” VPI-Aero-194, Virginia Polytechnic Institute & State University, 1993.

67. Landfield, J.P. and D. Rajkovic. “Canard/Tail Comparison for an Advanced Variable-Sweep-Wing Fighter,” *Journal of Aircraft*, Vol. 23, No. 6, June 1986, pp. 449-454.

68. Rech, Jean and Clive S. Leyman. *A Case Study by Aerospatiale and British Aerospace on the Concorde*, AIAA Professional Study Series.

69. Eberle, R.B., R.T. Stancil, and W.C. Fowler. “A Critical Review of Canard Relative To Aft Horizontal Tail Based on Low- and-High Speed Tunnel Tests of a Fighter/Attack Configuration,” AIAA-71-8, 1971.

70. Spearman, M. Leroy. “Effects of Wing and Tail Location on the Aerodynamic Characteristics of an Airplane for Mach Numbers From 0.25 to 4.63,” AIAA-80-1623, 1980.

71. Torenbeek, Egbert. *Synthesis of Subsonic Airplane Design*, Delft University Press, Delft, 1982.

72. Williams, John and Alice J. Ross. “Some Airframe Aerodynamic Problems at Low Speeds,” *Annals of the New York Academy of Sciences*, Vol. 154, Art.2, pp. 264-305, November 22, 1968.

73. Sachs, Gottfried. “Minimum Trim Drag and Optimum c.g. Position,” *Journal of Aircraft*, Vol. 15, No. 8, August 1978.

74. Nicholas, W.U., G.L. Naville, J.E. Hoffschwelle, J.K. Huffman, and P.F. Covell. “An Evaluation of the Relative Merits of Wing-Canard, Wing-Tail, and Tailless Arrangements for Advanced Fighter Applications,” ICAS-84-2.7.3, 1984.

75. Hutchison, Matthew G. “Multidisciplinary Design Optimization of High-Speed Civil Transport Configurations Using Variable-Complexity Modeling,” Ph.D. Dissertation, Virginia Polytechnic Institute & State University, March 1993.

76. Hutchison, M.G., E.R. Unger, W.H. Mason, B. Grossman, and R.T. Haftka. “Aerodynamic Optimization of an HSCT Configuration Using Variable-Complexity Modeling,” AIAA 93-0101, January 1993.

77. Hutchison, M.G., E.R. Unger, W.H. Mason, B. Grossman, and R.T. Haftka. “Variable-Complexity Aerodynamic Optimization of a High-Speed Civil Transport Wing,” *Journal of Aircraft*, Vol. 31, No. 1, pp. 110-116, January-February 1994.

Appendix A: Annotated Bibliography

This bibliography includes a brief description of what type of information is included in each paper. A brief description of the wind-tunnel model, test conditions, and tested parameters is also given for reports that are related to experimental investigations. The list of sources is organized by major topic, then alphabetically by author, and finally by year (most recent dates last). The major topics are:

Experimental Investigations of Supersonic Transports
Experimental Investigations Related to Supersonic Cruise Planforms
Theoretical Investigations
Configuration Design
Reference Reports
Control Issues

Note that this list is in no way complete and is concerned primarily, but not limited to, the longitudinal aerodynamic characteristics of supersonic cruise type planforms. This list is also not limited to sources cited in the report.

A.1 Experimental Investigations of Supersonic Transports

- Coe, Paul L., Jr., H. Clyde McLemore, and James P. Shivers. "Effects of Upper-Surface Blowing and Thrust Vectoring on Low-Speed Aerodynamic Characteristics of a Large-Scale Supersonic Transport Model," NASA TN D-8296, 1976.

AST-100 type configuration (74/70.5/60 sweep) powered model. Plotted force data. Tuft flow visualization. Leading and trailing edge flaps. Horizontal tail. Rounded leading-edge. Engines with deflectable nozzles mounted above the wing. Powered tests done in the Langley 30- by 60-Foot Full Scale Tunnel ($\alpha = -10^o$ to 34^o, $Re = 5.17x10^6$). Results include:

Flap effectiveness with engines on upper surface.
Flap effectiveness with engines mounted below wing.
Horizontal tail effectiveness.
Variation of thrust coefficient and nozzle deflection.
Discussions of performance and considerations of aircraft with these engine configurations.
Effect of sideslip and engine-out characteristics.
Effect of spoiler deflection.

- Coe, Paul L., Jr., Paul M. Smith, and Lysle P. Parlett. "Low Speed Wind Tunnel Investigation of an Advanced Supersonic Cruise Arrow-Wing Configuration," NASA TM 74043, 1977.

AST-100 type configuration (74/70.5/60 sweep) 0.045 dynamically scaled model. Plotted and tabulated force data. Krueger leading edge flap, trailing edge flaps. Horizontal tail. Rounded leading edges. Powered test done in Langley V/STOL Tunnel (α = -5^o to 25^o, Re = 2.5x10^6). Results of longitudinal and lateral/directional data include:

Effect of leading and trailing edge flap deflections.
Effect of thrust vectoring.
Horizontal tail effectiveness.
Effect of forebody strakes.

- Coe, Paul L., Jr. and Robert P. Weston. "Effects of Wing Leading-Edge Deflection on Low-Speed Aerodynamic Characteristics of a Low-Aspect-Ratio Highly Swept Arrow-Wing Configuration," NASA TP 1434, 1979.

AST-100 type configuration (74/70.5/60 sweep) dynamically scaled model. Plotted and tabulated force data. Tuft mast flow visualization. Krueger leading-edge flap. Segmented leading and trailing edge flaps (4 leading-edge segments). Horizontal tail. Rounded leading edge. Tested in the Langley V/STOL Tunnel (a = -10^o to 17^o, M = 0.07, Re = 2.0x10^6). Results of longitudinal and lateral/directional data includes:

Leading and trailing edge flap effectiveness with the goal of minimizing the formation of leading-edge vortices.
Horizontal tail effectiveness.
Aileron effectiveness.

- Coe, Paul L., Jr. and James L. Thomas. "Theoretical and Experimental Investigation of Ground-Induced Effects for a Low-Aspect-Ratio Highly Swept Arrow-Wing Configuration," NASA TP 1508, 1979.

AST-100 type configuration (74/70.5/60 sweep) dynamically scaled model. Plotted and tabulated force data. Segmented leading and trailing edge flaps (4 leading-edge segments). Horizontal tail. Rounded leading edge. Tested in the Langley V/STOL Tunnel (α = -2^o to 12^o, M = 0.07, Re = 2.0x10^6) with a moving ground plane. Results of ground induced effects includes:

Longitudinal stability.
Effects on performance.
Effect of horizontal and vertical tails.
Effect on landing/approach maneuver.
Comparison to numerical predictions.
Discussion of theory behind ground induced effects.

- Coe, Paul L, Jr., Jarrett K. Huffman, and James W. Fenbert. “Leading-Edge Deflection Optimization for a Highly Swept Arrow-Wing Configuration,” NASA TP 1777, 1980.

AST-100 type configuration (74/70.5/60 sweep) model. Plotted and tabulated force data. Includes input data set for numerical calculations. Segmented leading and trailing-edge flaps (12 leading-edge segments). Variable anhedral. No aft fuselage. Tested in the Langley 7- by 10-Foot Tunnel (α = -6^o to 15^o, M = 0.14, Re = 2.8 x 10^6). Longitudinal and lateral directional results include:

Effect of leading edge deflection (30^o deflection and optimized continuously varied deflection so that the leading edge is aligned with the local upwash along the span).
Effect of geometric anhedral.
Comparison to numerically predicted data.

- Coe, Paul L., Scott O. Kjelgaard, and Garl L. Gentry Jr. “Low Speed Aerodynamic Characteristics of a Highly Swept, Untwisted, Uncambered Arrow Wing,” NASA TP 2176, 1983.

AST-200 configuration 0.0359 scale model (74/70.5/60 sweep). Tabulated and plotted force data. Plotted pressure data for chordwise and spanwise stations. Single leading edge flap. Outboard vertical tails. No horizontal tail. Rounded leading edges. Tested at Langley 14- by 22-Foot Tunnel (α = -7^o to 17^o, M = 0.25, Re = 4.8 x 10^6). Results include:

Effectiveness of leading and trailing edge flap deflections on forces and pressures.
Effectiveness of various spoiler deflections on forces.
Vortex core locations for various angles-of-attack.
Comparison to VLM code results (includes numerical model input file).
Comparison of suction parameter and forces to cambered and twisted wing.

- Freeman, Delma C., Jr. and Richard D'Amato. “The Aerodynamic Characteristics of a Fixed Arrow Wing Supersonic Transport Configuration (SCAT 15F-9898) Part II - Stability Characteristics In the Deep Stall Angle of Attack Range,” NASA LWP-724, 1969.

SCAT-15F-9898 configuration 0.03 scale model. Plotted force data. Outboard vertical tails, leading edge notch, leading and trailing edge flaps, and canard. Tested in the Langley 30- by 60-Foot Full Scale Tunnel (α = -3^o to 62^o, Re = 3.92x10^6). Discussions are limited, results include:

Effect of leading edge radius.
Effect of wing apex notch.
Canard effectiveness.
Horizontal tail effectiveness.
Leading and Trailing-edge flap effectiveness.

- Lockwood, Vernard E. “Effect of Leading Edge Contour and Vertical-Tail Configuration on the Low-Speed Stability Characteristics of a Supersonic Transport Model a Having Highly-Swept Arrow Wing,” NASA TM 78683, 1978.

SCAT -15F configuration model (74/70.5/60 sweep). Plotted force data. Single leading edge flap. Outboard vertical tails. Horizontal tail. Forebody strake. Rounded leading edges. Tested at Langley High Speed 7- by 10-Foot Tunnel ($\alpha = 8^o$ to 32^o, M = 0.13, Re = $3.0x10^6$). Results include:

Effect of side-slip.
Effect of various leading edge radii.
Effect of vertical tail positions.
Effect of forebody strakes.

- McLemore, H. Clyde, Lysle P. Parlett, and William Sewall. “Low-Speed Wind-Tunnel Tests of 1/9-Scale Model of a Variable-Sweep Supersonic Cruise Aircraft,” NASA TN D-8380, 1977.

SCAT-16 configuration 1/9 scale model. Plotted force data. T-tail configuration. Inboard and outboard leading and trailing edge flaps. High horizontal tail. Rounded leading edge. Wing sweep varies from 20^o to 72^o. Tested at Langley 30- by 60-Foot Full-Scale Tunnel ($\alpha = -5^o$ to 36^o, Re = 3.92 to $5.95x10^6$). Results include:

Presentation of tuft flow patterns for 20^o sweep condition with variation of strake incidence, leading edge deflection, sideslip, and flow velocity.
Effects of Reynolds number, wing sweep, and horizontal tail position.
Effects of high lift devices.
Effects of various strake designs and strake leading edge devices.
Effect of horizontal tail incidence.

- McLemore, H. Clyde and Lysle P. Parlett. “Low-Speed Wind-Tunnel Tests of a 1/10-Scale Model of a Blended-Arrow Supersonic Cruise Aircraft,” NASA TN D-8410, 1977.

Blended fuselage low-boom concept aircraft configuration ($80^o/70^o$ continuous sweep) 0.10 scale powered model. Plotted force data. Tuft flow visualization. Low mounted canard. Segmented leading and trailing-edge flaps. Four centerline engines with vectored thrust nozzles. Fixed twin vertical tails, no horizontal tail. Powered tests done in the Langley 30- by 60-Foot Full Scale Tunnel ($\alpha = -6^o$ to 30o, Re = 6.78 to $13.85x10^6$). Longitudinal and lateral/directional results include:

Reynolds number effects.
Vertical tail effects.
Flap deflection effectiveness of varying flap deflection configurations.

Effects of canard, canard area, and incidence.
Thrust and thrust vectoring effects.
Sideslip effects and lateral/directional control characteristics.
Flap control effectiveness.

- Radkey, R.L., H.R. Welge, and J.E. Felix. "Aerodynamic Characteristics of a Mach 2.2 Advanced Supersonic Cruise Aircraft Configuration at Mach Numbers from 0.5 to 2.4," NASA CR 145094, 1977.

Douglas D3230-2.2-5E configuration 1.5% scale model ($71^o/57^o$ sweep). Single vertical tail, Krueger leading edge flaps. Horizontal tail. Table of wing and nacelle coordinates. Plotted force and pressure data (tabulated data is available on microfiche).Tuft, schlieren, and sublimation used for flow visualization. Tested at NASA Ames Unitary Plan Wind Tunnel, Ames 11-Foot transonic tunnel (M=0.5 to 1.3, $Re = 4.0x10^6$) and Ames 9- by 7-Foot Supersonic Tunnel (M=1.6 to 2.4, $Re = 4.0x10^6$). Main goal of the report was to build the database on this configuration. No flap deflection data other than Krueger flap is presented.

- Re, Richard J. and Lana M. Couch. "The Aerodynamic Characteristics of a Fixed Arrow Wing Supersonic Transport Configuration (SCAT 15F-9898) Part III - Reynolds Number Effects on the Stability Characteristics In the Deep Stall Angle of Attack Range," NASA LWP-735, 1969.

SCAT-15F-9898 configuration 0.03 scale model. Plotted and tabulated force data. Outboard vertical tails, leading edge notch, leading and trailing edge flaps, and canard. Tested in the Langley 16-Foot Transonic Tunnel ($\alpha = -10^o$ to 45^o, M = 0.13 to 0.27, $Re = 3.0$ to $5.94x10^6$). Discussions are limited, results include:

Effect of Reynolds number.
Effect of leading edge radius.
Effect of wing apex notch.
Canard effectiveness.
Horizontal tail effectiveness.
Leading-edge flap effectiveness.

- Shivers, James P., H. Clyde McLemore, and Paul L. Coe, Jr. "Low-Speed Wind-Tunnel Investigation of a Large-Scale Advanced Arrow-Wing Supersonic Transport Configuration with Engines Mounted Above Wing for Upper-Surface Blowing," NASA TN D-8350, 1976.

AST-100 type configuration (74/70.5/60 sweep) powered model with elastic wing construction. Plotted force data. Wake surveys. Trailing edge flaps with blowing. With and without horizontal T-tail. Rounded leading-edge. Engines with exhaust deflectors mounted

above the wing. Powered tests done in the Langley 30- by 60-Foot Full Scale Tunnel (α = -10^o to 32^o, Re = 3.53 to 7.33x10^6). Results include:

Horizontal tail characteristics.
Downwash characteristics.
Pitch trim considerations and performance issues.
Lateral/directional control and engine-out characteristics.
Effect of exhaust deflection.

- Smith, Paul. "Low-Speed Aerodynamic Characteristics from Wind-Tunnel Tests of a Large-Scale Advanced Arrow-Wing Supersonic Transport Concept," NASA CR 145280, 1978.

AST-100 type (74/70.84/60 sweep) configuration. Plotted and tabulated force data. Horizontal tail. Forebody strakes. Two inboard leading edge flaps and trailing edge flaps. One outboard leading edge flap and trailing edge flap/aileron. Rounded leading edge (0.68%c leading edge radius). Tested at the Langley 30- by 60-Foot Full Scale Tunnel (α = -10^o to 25^o, Re = 5.88 x 10^6). Results for longitudinal and lateral/directional characteristics include:

Leading edge flap effectiveness
Trailing edge flap effectiveness.
Horizontal tail effectiveness.
Fore-body strake effectiveness.

- Yip, Long P. and Lysle P. Parlett. "Low-Speed Wind-Tunnel Tests of a 1/10-Scale Model of an Arrow-Wing Supersonic Cruise Configuration Designed for Cruise at Mach 2.2," NASA TM 80152, 1979.

McDonnell Douglas supersonic transport configuration (71^o/57^o sweep) 0.10 scale model. Plotted and tabulated force data. Plotted pressure data. Tuft flow visualization. Horizontal tail. Segmented leading and trailing edge flaps (6 leading edge flap segments). Rounded leading edge. Tested in the Langley 30- by 60-Foot Full Scale Tunnel (a = -6^o to 23^o, M = 0.09, Re = 4.0x10^6). Results for longitudinal and lateral/directional data include:

Flow visualization studies.
Evaluation of pressure distributions.
Effect of segmented leading edge flap.
Effect of trailing edge flaps.
Horizontal tail effectiveness.
Sideslip effects.
Lateral/directional control characteristics.

A.2 Experimental Investigations Related to Supersonic Cruise Planforms

- Bradley, R.G., W.O. Wray, and C.W. Smith. "An Experimental Investigation of Leading-Edge Vortex Augmentation by Blowing," NASA CR-132415, 1974.

Testing of six 30^o and 45^o sweep diamond, arrow and delta wing models. Blowing on the upper surface was used to investigate the effects on vortex breakdown. Plotted and tabulated data. Oil flow visualization. Tests were conducted in the General Dynamics 8- by 12-Foot Low Speed Wind Tunnel ($\alpha = -2^o$ to 34^o, M = 0.2, Re = 7.0×10^6). The following investigations were made:

Nozzle position.
Variation of momentum coefficient.

- Grafton, Sue B. "Low-Speed Wind-Tunnel Study of the High-Angle-of-Attack Stability and Control Characteristics of a Cranked-Arrow-Wing Fighter Configuration," NASA TM 85776, 1984.

Modified 0.15 scale F16A model to represent F-16XL configuration ($70^o/50^o$ sweep). Plotted force data. Smoke flow visualization. With and without leading edge notch. Trailing edge extension. Wing fences. No control surfaces. Tailless configuration. Tested in the Langley 30- by 60-Foot Full Scale Tunnel ($\alpha = -4^o$ to 41^o, M = 0.07, Re = 2.15×10^6). Longitudinal and lateral/directional results include:

Apex notch modification effects.
Fence and fence modification effects.
Trailing edge extension effects.

- Grafton, Sue B. and Luat T. Nguyen. "Wind-Tunnel Free-Flight Investigation of a Model of a Cranked-Arrow-Wing Fighter Configuration," NASA TP 2410, 1985.

F16XL configuration ($70^o/50^o$ sweep) 0.18 scale model. Plotted force data. Smoke flow visualization. Static and dynamic force tests were conducted along with powered free-flight tests. Leading and trailing edge flaps (no inboard leading edge flaps other than added on vortex flaps). Tested in the Langley 30- by 60-Foot Full Scale Tunnel ($\alpha = 0^o$ to 40^o, Re = 2.15×10^6). Longitudinal and lateral/directional results include:

Effects of elevon and aileron deflection.
Effect of leading edge flaps and speed brakes.
Effects of vortex flaps.
Sideslip effects.
Presentation of dynamic derivatives.
Flight characteristics.

- Johnson, Joseph L., Jr., Sue B. Grafton, and Long P. Yip. "Exploratory Investigation of the Effects of Vortex Bursting on the High Angle-of-Attack Lateral-Directional Stability Characteristics of Highly-Swept Wings," AIAA 11th Aerodynamic Testing Conference. AIAA 80-0463, 1980.

Tests of a collection of wings (flat plate 70^o delta with sharp leading edges, 70^o arrow wing-fuselage combination, and several 70^o arrow wing flat plate models of different sizes). Lateral/directional test results include:

Test configuration, including model support interference and tunnel configuration.
Wing fence effects.
Vertical tail location effects.

- Lamar, John E. and Jay Brandon. "Vortex Features of F-106B Aircraft at Subsonic Speeds," 11th AIAA Applied Aerodynamics Conference. AIAA-93-3471, 1993.

Flight study of the vortex flow on the F-106B aircraft in 1-g flight. Methods include vapor screen, image enhancement, photogrammetry, and computer graphics. Plotted location of flow separation and reattachment, and vortex cores. Comparison of results to wind-tunnel data.

- Marsden, D.J., R.W. Simpson, and W.J. Rainbird. "The Flow Over Delta Wings at Low Speeds with Leading-Edge Separation," The College of Aeronautics, Cranfield. Report No. 114, 1958.

Presentation of vortex flow over two delta wings of 60 and 70 degree sweep. Oil flow, smoke flow, flowfield surveys, and pressure plots are presented. Vortex core position (height and spanwise location) is also plotted. Description of vortex flow structure.

- Nelson, C.P. "Effects of Wing Planform On HSCT Off-Design Aerodynamics," AIAA-92-2629-CP.

Presentation on development of supersonic cruise planforms and the effects of planform on the aerodynamic characteristics. Test of three typical supersonic cruise planforms which represent a parametric study of the Boeing B2707-300 planform. Off-design studies of 1.5% scale models were tested in a 12x8 foot transonic tunnel include:

Plotted force data is presented without actual values to preserve proprietary information.
Oil flow visualization.
Discussion of subsonic pitch-up.
Effects of planform and airfoil on aerodynamics.

- Quinto, P. Frank and John W. Paulson. “Flap Effectiveness on Subsonic Longitudinal Aerodynamic Characteristics of a Modified Arrow Wing,” NASA TM 84582, 1983.

Untwisted, uncambered modified arrow wing (70/48.8 sweep) with NACA 0004 airfoil section. Plotted and tabulated force data. Segmented leading and trailing edge flaps. No horizontal tail. Tested at the Langley 4- by 7-Meter Tunnel (α = -4^o to 20^o, M = 0.2, Re = 4.5x10^6). Results include:

Trailing edge flap effectiveness.
Effect of leading edge flaps.
Combined effects of flaps.
Comparison to theoretical predictions.

- Rao, Dhanvada M. and Thomas D. Johnson, Jr. “Subsonic Pitch-up Alleviation on a 74 Deg Delta Wing,” NASA CR 165749, 1981.

Flat plate 74o sweep delta wing with blunt leading edges. Pylon Vortex Generators were used to reduce the leading edge flow separation thus reducing the pitch-up at high angles of attack without increasing the induced drag. Tested at the Langley 7- by 10-Foot High Speed Wind-Tunnel (M = 0.2, Re = 2.7 x 10^6). Plotted force data, tabulated data available in NASA CR 159120.

- Rao, Dhanvada M. “Exploratory Investigation of a Tip Blowing Concept on a Cranked-Arrow ‘HSCT' Planform,” AIAA-92-2637, 1992.

Test of a 70o/50o sweep flat plate model with sharp leading edges. Blowing on the outer wing section was incorporated to prevent pitch-up and for roll control at high angles of attack. Smoke flow, oil flow, pressure plots, and force plots are presented.

- Shah, Gautam H. “Wind-Tunnel Investigation of Aerodynamic and Tail Buffet Characteristics of Leading-Edge Extension Modifications to the F/A-18,” AIAA Atmospheric Flight Mechanics Conference. AIAA 91-2889, 1991.

Test of a 0.16 scale model of an F/A-18 with rigid and flexible vertical tails. Plotted static and dynamic forces and smoke flow visualization of vortex flow. Report includes discussions on effect of modifications of leading-edge extensions on vortex flow and interactions with vertical tails along with flow with fences and extension removed.

- Smith, Donald W., Harry H. Shibata, and Ralph Selan. “Lift, Drag, and Pitching Moment of Low-Aspect-Ratio Wings at Subsonic and Supersonic Speeds - An Investigation at Large Reynolds Numbers of the Low Speed Characteristics of Several Wing-Body Combinations,” NACA RM A51K28, 1952.

Investigation of a series of wings with twist and camber tested at low speeds. Planforms tested were deltas, cropped arrows, and cropped diamond configurations. No control

surfaces. Tested in the Ames 12-Foot Pressure Tunnel (α = -1^o to 28^o. M = 0.25, Re = 2.4 to 16.6x10^6) and the Ames 6- by 6-Foot Supersonic Tunnel (α = -1^o to 16^o, M = 0.6, Re = 2.4 to 3.1 x10^6). Only aerodynamic data is presented, no analysis. Summary plots of all the configuration is included.

- Wentz, William H., Jr. "Wind Tunnel Investigations of Vortex Breakdown on Slender Sharp-Edged Wings," Ph.D. Thesis, University of Kansas, 1968 (also NASA CR 98737 with David L. Kohlman).

Experimental study of the effects of planform on leading edge vortex breakdown. All models were flat plates with wedge shaped leading edges. All tests were done at the University of Kansas low-speed tunnel (q = 30 psf, Re = 1.0x106). Plotted data of forces and vortex core breakdown position. Schlieren system used for flow visualization.

A.3 Theoretical Investigations

- Carlson, Harry W., Robert J. Mack, and Raymond L. Barger. "Estimation of Attainable Leading-Edge Thrust for Wings at Subsonic and Supersonic Speeds," NASA TP 1500, 1979.

Theoretical description of the calculation of the attainable thrust of a wing at subsonic speeds as implemented in a vortex lattice code. Description of the development of the method from empirical relations. Analysis of a variety of wings and comparison to experimental data.

- Carlson, Harry W. and Kenneth B. Walkley. "A Computer Program for Wing Subsonic Aerodynamic Performance Estimates Including Attainable Thrust and Vortex Lift Effects," NASA CR 3515, 1982.

Description of the methods used in a computer program to predict the aerodynamic characteristics of wings in subsonic flow. Includes attainable thrust calculations and camber and twist solution incorporation by means of superposition. Vortex lattice method solved my means of perturbation velocity iteration. Comparisons to experimental data.

- Carlson, Harry W. and Kenneth B. Walkley. "An Aerodynamic Analysis Computer Program and Design Notes for Low Speed Wing Flap Systems," NASA CR 3675, 1983.

Modifications to the code described in NASA CR 3515 to include the capability to simply analyze flap systems. Also incorporates an improved method for calculating the attainable thrust and further options for the calculation of the vortex lift. Comparisons to experimental data.

- Carlson, Harry W. and Kenneth B. Walkley. “Numerical Methods and a Computer Program for Subsonic and Supersonic Aerodynamic Design and Analysis of Wings With Attainable Thrust Considerations,” NASA CR 3808, 1984.

Description of a computer code which incorporates the theories developed in NASA CR 3515 and CR 3675. Includes:

Basic theory used for the program.

Detailed description of the options for the calculation of the vortex lift.

Description of the wing design process used by the code.

Detailed description in the use of the code including program application.

- Carlson, Harry W. “The Design and Analysis of Simple Low Speed Flap Systems With the Aid of Linearized Theory Computer Programs,” NASA CR 3913, 1985.

Description of a method to design flap systems with the use of the codes described in NASA CR 3808 and CR 3675. Description of the principle behind the method. Design and analysis of a candidate flap system with effects of leading edge radius, flap segmentation, vortex force, and Reynolds number being taken into consideration. Comparison to experimental data.

- Carlson, Harry W. and Christine M. Darden. “Applicability of Linearized-Theory Attached-Flow Methods to Design and Analysis of Flap Systems at Low Speeds for Thin Swept Wings With Sharp Leading Edges,” NASA TP 2653, 1987.

Application of the code described in NASA CR 3913 in the design and analysis of a wider variety of configurations and flow conditions for validation of the code. Comprehensive set of data correlation with experimental data. Description of design methodology. Sample input files included.

- Carlson, Harry W. and Christine M. Darden. “Validation of a Pair of Computer Codes for Estimation and Optimization of Subsonic Aerodynamic Performance of Simple Hinged-Flap Systems for Thin Swept Wings,” NASA TP 2828, 1988.

More extensive study of the code used in NASA TP 2653 in the design and analysis of flap systems. A wider variety of planforms is used in this study which includes comparisons to experimental data. Description of flap performance considerations and detailed analysis of a set of configurations is presented. Detailed description of the use of the WINGDES2 computer code is presented with sample input files.

● Carlson, Harry W., Christine M. Darden, and Michael J. Mann. “Validation of a Computer Code for Analysis of Subsonic Aerodynamic Performance of Wings With Flaps in Combination With a Canard or Horizontal Tail and an Application to Optimization,” NASA TP 2961, 1990.

Description of the modifications made to the code described in NASA CR 3675 to allow for two surfaces to analyzed. Complete description of the use of the AERO2S code including sample input and output files. Analysis of a variety of configurations and comparison to experimental data. Examples of configuration optimization. Description of code applications and limitations.

● Carlson, Harry W. and Michael J. Mann. “Survey and Analysis of Research on Supersonic Drag-Due-to-Lift Minimization With Recommendations for Wing Design,” NASA TP 3202, 1992.

Description of the use of the code described in NASA CR 3808 in the calculation of the aerodynamic performance of wings in supersonic flow with empirical corrections to more closely approximate the attainable leading edge thrust. Discussion of theoretical wing design, theoretical methods used in the code, and the application and guidelines of the empirical methods. Analysis of a variety of wings and comparisons to experiment. Comparison of results with output from Euler code analyses. Complete description of the use of the code WINGDES2 and sample input and output files.

● Lamar, John, E. “Extension of Leading-Edge Suction Analogy to Wings with Separated Flow Around the Side Edges at Subsonic Speeds,” NASA TR-R-428, 1974.

Discussion of the theory involved in predicting the side edge vortex force used in a vortex lattice code. Example theoretical and experimental cases. Comparison of theoretical results with experiment. and other theories. Force plots on a variety of flat wings.

● Lamar, John E. and Blair B. Gloss. “Subsonic Aerodynamic Characteristics of Interacting Lifting Surfaces with Separated Flow Around Sharp Edges Predicted by a Vortex Lattice Method,” NASA TN D-7921, 1975.

Discussion of the theory in predicting the leading and side edge vortex forces incorporated in the vortex lattice code (NASA TM 83303). Sample input file and comparison to experiment is presented.

- Lamar, John E. "Recent Studies of Subsonic Vortex Lift Including Parameters Affecting Stable Leading-Edge Vortex Flow," *Journal of Aircraft*, Vol.14, no. 12, December 1977.

Discussion of augmented lift effects and the implementation of the theory into a vortex lattice code. Include comparisons with experimental data. Includes plotted force data, oil flow photographs, and figures of vortex system.

- Lamar, John E. "Analysis and Design of Strake-Wing Configurations," *Journal of Aircraft*, Vol. 17, no. 1, January 1980.

Analysis and design of straked-wing configurations with the goal of improving high angle of attack aerodynamic characteristics. Includes a theoretical analysis and experimental testing of a variety of configurations. Plotted force data, oil flow photographs, and discussion of theory involved in analysis.

- Lamar, John E. and Henry E. Herbert. “Production Version of the Extended NASA-Langley Vortex Lattice FORTRAN Computer Program - Volume I - User's Guide,” NASA TM 83303, 1982.

User's manual for vortex lattice code which includes the prediction of leading and side edge vortex forces. Includes example input and output files but does not include a discussion of the theories incorporated in the code. Volume II is also available which contains a listing of the source code.

- Lan, C.E. and C.H. Hsu. “Effects of Vortex Breakdown on Longitudinal and Lateral-Directional Aerodynamics of Slender Wings by the Suction Analogy,” AIAA 9th Atmospheric Flight Mechanics Conference. AIAA-82-1385, 1982.

Incorporation of vortex breakdown in a vortex lattice code in predicting the high angle of attack aerodynamic characteristics is presented. Report includes:

Comparison to experimental data of a variety of delta, modified delta, and cranked delta planforms (plotted force data).
Discussion of the development of the theory.
Vortex breakdown empirical correlation includes vortex breakdown in sideslip and rolling.
Incorporation of side-edge lift.

A.4 Configuration Design

- Antani, D.L. and J.M. Morgenstern. “HSCT High-Lift Aerodynamic Technology Requirements,” AIAA-92-4228. Aircraft Design Systems Meeting, 1992.

Discussion of the impact of high-lift aerodynamics on:

Noise constraints.
Take-off/landing requirements.
Discussion of past methods and research areas. Discussion of current and future technology, research areas, and future requirements.

- Barber, Hal T., Jr. and E.E. Swanson. “Advanced Supersonic Technology Concept AST-100 Characteristics Developed in a Baseline-Update Study,” NASA TM X-72815, 1976.

Complete design study of the AST-100 configuration developed from the baseline concepts from 1973. Full report includes wind-tunnel data from NASA Langley Full Scale Tunnel and Ames 12-Foot Pressure Tunnel. Advancements from baseline include reduction of wing thickness, nacelle resizing, improvement in lift-to-drag ratios, and resized rudder developed from lateral-directional study not previously available.

- Barber, Hal T. “Characteristics of the Advanced Supersonic Technology AST-105-1 Configured for Transpacific Range with Pratt and Whitney Aircraft Variable Stream Control Engines,” NASA TM 78818, 1979.

Configuration description of the AST-105-1 developed from tests on the AST-100. Analysis and design of the configuration is based on theoretical predictions and an aerodynamic database.

Includes tabulated and plotted low speed lift and drag and high speed drag polars. Tabulated and plotted control effectiveness. Figures of configuration. Report includes description of:

Low and high-speed aerodynamics.
Stability and control.
Stability augmentation.
Dynamic stability developed from flight simulator "flights."
Propulsion including engine description, nacelle design, and performance.
Mass properties.
Environmental factors including noise and sonic boom.
Mission analysis including requirements, propulsion constraints and off-design operation.
Economics.

- Barber, Hal T., Jr. “Characteristics of an Advanced Supersonic Technology Transport (AST-106-1) Configured with Variable-Cycle Engines for Transpacific Range,” NASA TM 81879, 1982.

Theoretical design of AST-106-1 configuration. Report is mainly concerned with applying more recent analysis methods to the AST-105-1 design while incorporating new technologies. Estimates for aerodynamic performance incorporate analysis methods along with wind tunnel data. The report includes:

Low-speed and high-speed aerodynamic assessment.
Presentation of stability and control criteria and control surface configuration.
Presentation of variable-cycle engine and performance.
Mass characteristics.
Discussion of environmental factors including noise and sonic boom.
Presentation of mission analysis requirements and sizing constraints
Economic market analysis.

- Douglas Aircraft Company. “Study of High-Speed Civil Transports,” NASA CR 4236, 1990.

HSCT Systems study including:

Market analysis.
Vehicle concepts assessment (from Mach 2.0 to 25) including engine selection.
Mission analysis including economics and performance.
Environmental aspects (noise and sonic boom).
Airport compatibility and requirements.
Future recommendations.

- Douglas Aircraft Company. “1989 High-Speed Civil Transport Studies,” NASA CR 4375, 1991.

Follow-up from CR 4236. Includes more information on sonic boom minimization, noise reduction, studies on engine emissions and laminar flow control. Includes future recommendations and a brief configuration description.

- Kehrer, W.T. “Design Evolution of the Boeing 2707-300 Supersonic Transport, Part II - Design Impact of Handling Qualities Criteria, Flight Control Systems Concepts, and Aeroelastic Effects on Stability and Control,” AGARD CP-147, Oct. 1973.

Report includes:

Impact of stability and control issues on configuration design includes stability augmentation system and horizontal tail sizing.
Aeroelasticity issues relative to configuration design and design cycle.
Report includes only summary plots of previous tests.

- Robins, A. Warner, Samuel M. Dollyhigh, Fred L. Beissner, Jr., Karl Geiselhart, Glenn L. Martin, E.W. Shields, E.E. Swanson, Peter G. Coen, and Shelby J. Morris, Jr. "Concept Development of a Mach 3.0 High-Speed Civil Transport," NASA TM 4058, 1988.

Concept description of the AST3I Mach 3.0 configuration. Configuration layout, mass properties, aerodynamics, propulsion, performance, and sizing. Predictions of zero-lift drag, induced drag, maximum lift-drag ratio and stability predictions are included. Also includes water tunnel test flow visualization photographs showing the vortex system present with pylon vortex generators/leading edge-notch flap.

- Swan, W.C. "Design Evolution of the Boeing 2707-300 Supersonic Transport, Part I - Configuration Development, Aerodynamics, Propulsion, and Structures," AGARD CP-147, Oct. 1973.

Report includes:

History of SST program.
Presentation of configuration aerodynamics.
Propulsion systems including engine placement and propulsion integration aerodynamics.
Structural concepts including material selection, dynamic analysis and flutter.
Preliminary design issues.
Report includes only summary plots of previous tests.

- Walkley, Kenneth B. and Glenn L. Martin. "Aerodynamic Design and Analysis of the AST-200 Supersonic Transport Configuration Concept," NASA CR 159051, 1979.

AST-200 configuration. Design of the configuration from the baseline AST-102. Description of numerical model used is presented for AST-102 and AST-200. Design considerations include:

Nacelle design.
Wing thickness development.
Wing twist and camber design.
Wing-body integration and wave drag optimization.
Numerical aerodynamic analysis includes:
Comparison of forces and moments between AST-102 and AST-200.

- Walkley, K.B., G.J. Espil, W.A. Lovell, G.L. Martin, and E.E. Swanson. "Concept Development of a Mach 2.7 Advanced Technology Transport Employing Wing-Fuselage Blending," NASA CR 165739, 1981.

Theoretical design and analysis of the AST-205 configuration. Results include:

Description of full configuration development from mission requirements.
Propulsion system description including nacelle design, engine size, and installed performance.

Presentation of mass properties including inertias.
Low speed aerodynamic data and stability and control taken from previous AST-105-1 tests and analyses.
High speed aerodynamics presented includes only drag polars as a function of Mach number.
Criteria for sizing and mission analysis is presented.

A.5 Reference Reports

- Hoffman, Sherwood. "Bibliography of Supersonic Cruise Research (SCR) Program from 1972 to Mid-1977," NASA RP 1003, 1977.
- Hoffman, Sherwood. "Bibliography of Supersonic Cruise Research (SCR) Program from 1977 to Mid-19"80," NASA RP 1063, 1980.
- Hoffman, Sherwood. "Bibliography of Supersonic Cruise Research (SCR) Program from 1980 to 1983," NASA RP 1117, 1984.

Gives a history of the SCAR program and a compilation of abstracts. Does not list reports on research applicable to HSCT configurations that were not specifically part of the SCAR program.

- Kulfan, R.M. "Wing Geometry Effects on Leading Edge Vortices," AIAA-79-1872. Aircraft Systems and Technology Meeting, 1979.

Theoretical and Experimental study of wing geometry effects on vortex flow and resulting forces. Plotted force and pressure data along with highly descriptive figures of flowfield, forces and vortex characteristics. Discussions and results include:

Formation and characteristics of vortex flow on sharp, slender wings.
Previous prediction methods for vortex flow and a description of the suction analogy used for theoretical predictions.
Airfoil shape effects (pointed and round-nose leading edges).
Warped wings.
Drag predictions.

Purely theoretical wing planform effects study (supported by previous experimental data) including sweep, notch ratio, taper ratio, twist, camber, nose radius, and flap effects.

- Lamar, John E. "High Angle of Attack - Aerodynamics. AGARD Special Course on Engineering Methods in Aerodynamic Analysis and Design of Aircraft," AGARD Report 783, 1992.

A comprehensive summary of theoretical prediction methods of high angle of attack aerodynamics of aircraft. The report includes methods from a variety of researchers in the following topics:

Vortex flow characteristics prediction methods
Discussion of design methods and use of prediction methods for high angle of attack flow in design methods.
Analysis methods of predicting stability and control characteristics.
Post stall flight characteristics including possible solutions.

- Poisson-Quinton, P. "Slender Wings for Civil and Military Aircraft." Eighth Theodore von Karman Memorial Lecture, *Israel Journal of Technology*, Vol. 16, No. 3, pp 97-131, 1978.

A comprehensive summary of the aerodynamic characteristics of slender wings. Includes many descriptive figures on each topic. Discussions include:

Vortex lift including theoretical predictions, flow visualization, vortex burst, and pitch-up.
Vortex control, vortex flaps, effect of leading edge contour and blowing on vortex lift, and strake effects.
Variable geometry wings including variable sweep canards.
Design for supersonic cruise.
Design for hypersonic cruise and reentry flight.

- Spearman, Leroy M. "The Evolution of the High-Speed Civil Transport," NASA TM 109089, 1994..

The history of the various programs involving supersonic transport is presented. Description of the major research and configurations studied during each program and reasons for the demise of each program.

- Spreeman, Kenneth P. "Design Guide for Pitch-Up Evaluation and Investigation at High Subsonic Speeds of Possible Limitations Due to Wing-Aspect-Ratio Variations," NASA TM X-26, 1959.

A design guide is given for wing-body and wing-body-tail combinations for design of configurations so as not to experience pitch-up. The study does not predict where pitch-up will occur, rather, it only predicts if pitch-up will occur. Discussion of the limitations of the method when applied to aircraft design. Tests are limited to delta planforms only. Analysis and experimental tests of varying aspect ratio wing-bodies was performed and is presented. Limited test data is presented. Plotted force data for varying Mach number. A extensive list of references on tests relevant to this subject is presented.

A.6 Control Issues

- Campbell, George S. and Joseph Weil. “The Interpretation of Nonlinear Pitching Moments in Relation to the Pitch-Up Problem,” NASA TN D-193, 1959.

Methods to calculate the longitudinal response of aircraft to control inputs with the use on non-linear data is presented. A study of the factors affecting and correcting pitch-up during flight is also presented. Plotted time histories of forces and aircraft motion is included.

- James, Harry A. and Lynn W. Hunton. “Estimation of Incremental Pitching Moments Due to Trailing-Edge Flaps on Swept and Triangular Wings,” NACA TN 4040, 1957.

Method of determining Cm-delta for swept wings from two-dimensional data is presented. Method seems to work with a fair amount of accuracy for the wings tested, although 2-D data is required for the wing sections. Method was tested for low angles of attack only. An extensive reference list of sources of two-dimensional airfoils and wing/wing-body tests is presented.

- McCarthy, Craig A., John B. Feather, John R. Dykman, Mark A. Page, and John Hodgkinson. “Design and Analysis Issues of Integrated Control Systems for High-Speed Civil Transports,” NASA CR 186022, 1992.

Identification of the issues for guidance and control systems for the HSCT aircraft. Discussion of the stability and control characteristics of HSCT aircraft, analysis of current technologies, and identification of current control systems problems and requirements. Discussion of the following issues includes identification of the characteristics, control requirements, and control design technology:

Pitch and directional stability and control.
Aeroelastic effects and acoustics.
Airframe propulsion interaction.

- Wolowicz, Chester H. and Roxanah B. Yancey. “Summary of Stability and Control Characteristics of the XB-70 Airplane,” NASA TM X-2933, 1973.

Description of the stability and control characteristics of the XB-70-1 determined from flight data. Some explanation of the discrepancies between flight and predictions. Plotted force and time history data. Discussions include:

Description of the control system and instrumentation..
Propulsion system.
Longitudinal char. including takeoff/landing, trim, control, and dynamic stability.
Lateral directional characteristics including landing, static stability and control, handling problems in sideslip, dutch-roll, aileron response and flight augmentation system.

Appendix B: Summary of Experimental Studies

A summary of the reports that deal with experimental studies of HSCT planforms or HSCT related tests is shown in Tables 1 and 2. Reports are listed by their report numbers.

Table B1 - Experimental studies of swept wing planforms

Reference	Sweep	Camber Twist	M Re ($x10^6$)	α (deg)	Force	Press.	Flow Vis.	Flaps	H. Tail	Comments
TM-85776	70/50	-	0.07 2.15	-4 to 41	Plot	-	Smoke	-	-	-
TP-2410	70/50	Twist	- 2.15	0 to 40	Plot	-	Smoke	LE TE	-	-
Cranfield No. 114	60 and 70	-	- -	-	Plot	Plot	Oil Smoke	-	-	-
AIAA-92-2629	75/50.5 76/68/48	-	- -	-	Plot	-	Oil	-	Low	-
TM-84582	70/48.8	-	0.2 4.5	-4 to 20	Plot/ Table	-	-	SLE TE	-	-
CR-165749	74	-	0.2 2.7	0 to 32	Plot	-	-	-	-	Vortex Generators
AIAA-92-2637	70/50	-	0.06 0.8	0 to 20	Plot	Plot	Oil Smoke	-	-	Blowing
RM-A51K28	Various	-	0.25-0.6 2.4-3.1	-1 to 28	Plot	-	-	-	-	-
CR-98737	Various	-	0.14 1.0	0 to 60	Plot	-	Schlieren	-	-	-
CR-132415	30 and 40	-	0.2 7.0	-2 to 34	Plot/ Table	-	Oil	-	-	Blowing

A key of the symbols used in the table is as follows:

LE: Leading-edge flap

TE: Trailing-edge flap

SLE(X): Segmented leading-edge flap where X = number of segments

KLE: Krueger flap on outboard wing section

"-": item is not included or information was not provided

Table B2 - Experimental studies of HSCT configurations.

Reference	Sweep	Camber Twist	M Re ($x10^6$)	α (deg)	Force	Press.	Flow Vis.	Flaps	H. Tail	Comments
TND-8296	74/70.5/60	Both	- 5.17	-10 to 34	Plot	-	Tuft	LE TE	Low	Powered
TM-74043	74/70.5/60	Both	- 2.5	-5 to 25	Plot/ Table	-	-	KLE TE	Low	Powered
TP-1434	74/70.5/60	Both	0.07 2.0	-10 to 17	Plot/ Table	-	Tuft Mast	SKLE(4) TE	Low	-
TP-1508	74/70.5/60	Both	0.07 2.0	-2 to 12	Plot/ Table	-	-	SLE(4) TE	Low	Ground Plane
TP-1777	74/70.5/60	Both	0.14 2.8	-6 to 15	Plot/ Table	-	-	SLE(12) TE	Low	Variable Anhedral
TP-2176	74/70.5/60	-	0.25 4.8	-7 to 17	Plot/ Table	Plot	-	LE	Low	-
LWP-724	74/70.5/60	Both	- 3.92	-3 to 62	Plot	-	-	LE TE	Low	Canard LE Notch
TM-78683	74/70.5/60	Both	0.13 3.0	8 to 32	Plot	-	-	LE	Low	Strake
TND-8380	20 to 72 Var. Sweep	Both	- 3.92-5.95	-5 to 36	Plot	-	-	LE TE	Low T-tail	-
CR-145280	71/57	Both	0.5-2.4 4.0	varies	Plot	Plot	Tuft Schlieren	KLE	Low	-
LWP-735	74/70.5/60	Both	0.13-0.27 3.0-5.94	-10 to 45	Plot/ Table	-	-	LE TE	Low	Canard LE Notch
TND-8350	74/70.5/60	Both	- 3.53-7.33	-10 to 32	Plot	-	-	TE	T-tail	Blowing Powered
CR-145280	74/70.5/60	Both	- 5.88	-10 to 25	Plot/ Table	-	-	LE TE	Low	Strakes
TM-80152	71/57	Both	0.09 4.0	-6 to 23	Plot/ Table	Plot	Tuft	SLE(6) TE	Low	-
TND-8410	80/70 Cont.	Both	- 6.78-13.85	-6 to 30	Plot	-	Tuft	SLE TE	-	Canard Powered

A key of the symbols used in the table is as follows:

LE: Leading-edge flap

TE: Trailing-edge flap

SLE(X): Segmented leading-edge flap where X = number of segments

KLE: Krueger flap on outboard wing section

"-": item is not included or information was not provided

Appendix C: Instructions for the Implementation of the APE Method

The aerodynamic pitch-up estimation method (APE) uses the vortex lattice method code named *Aero2s* (January 1994 version), developed by Dr. Harry Carlson, to estimate the inviscid aerodynamic characteristics along with estimates for the thrust and vortex forces. The APE method is simply an extension of this code and only requires an additional two variables to the input file. To differentiate this code from the original *Aero2s*, it was named *Aero2s2*. For instructions on the use of the code, reference 29 should be used along with these notes. The code is run in the same manner as is described in ref. 29. To execute the code, the command is:

`aero2s2 < input > output`

where:

input - input file name

output - output file name (screen output is used if no name is specified)

The two additional variables which should be included in the NAMELIST input file are:

CLMAX - value of the maximum 2-D lift coefficient for the outboard wing panel airfoil section (default = 10.0).

CRANK - y location of the wing crank as a fraction of the wing semi-span (default = 1.0).

These values may be specified anywhere in the NAMELIST input file. The output file is as is described in ref. 29. In addition, three other output files are generated, they are:

pressout.dat - This is a file containing the configuration geometry and pressure data. This file is in a *TecPlot* input file format and the data is arranged in a mesh format for the generation of pressure contour plots. Three options are available and are chosen with the use of a specifier of the IPRCPD variable in the input file. The options are:

IPRCDP = 1 - Total pressure values are plotted (before the APE correction)

2 - Inviscid solution only (before APE)

3 - Vortex pressures only

cloutb.dat - Lift, drag and moment as a function of alpha. No header is included for this file. Seven columns are generated, the first column is the angle of attack in degrees. The next three columns are lift, drag, and pitching moment coefficients without the APE correction. The final three columns are lift, drag, and pitching moment coefficients of the inviscid solution only without the APE correction.

cloutc.dat - Same as the above file except that the first set of coefficients are for the aerodynamic coefficients calculated with the APE method and the final three columns are the aerodynamic coefficients without the APE correction.

The APE output is only contained in the cloutc.dat file. Finally, the only change to the original operation of the *Aero2s* code was the limit imposed on the vortex forces. The vortex effects were omitted for spanwise stations that were inboard of the YAPEX specifier. It should be noted that there was a large degree of sensitivity associated with the proper selection of the YAPEX value. This was true before and after the modification of "limiting" the vortex. There is no option to eliminate the vortex limiting modification, this is a permanent change to *Aero2s*.